

15. CORE-LOG INTEGRATION OF NATURAL GAMMA RAY INTENSITY TO CONSTRUCT A 10-M.Y. CONTINUOUS SEDIMENTARY RECORD OFF SANRIKU, WESTERN PACIFIC MARGIN, ODP SITES 1150 AND 1151¹

Tatsuhiko Sakamoto,² Saneatsu Saito,³ Chieko Shimada,⁴ and Masayuki Yamane⁵

ABSTRACT

Detection of climate response to orbital forcing during Cenozoic long-term global cooling is a key to understanding the behavior of Earth's icehouse climate. Sedimentary rhythm, which is a rhythmic or cyclic variation in the sequence of sediments and sedimentary rocks, is useful for quantitative reconstruction of Earth's evolution during geological time. In this study, we attempt to (1) identify sources of natural gamma ray (NGR) emissions of core recovered during Ocean Drilling Program (ODP) Leg 186 by analyses of physical properties, major element concentrations, diatom abundances, and total organic carbon contents, (2) integrate whole-core NGR intensity of recovered core with wireline logging NGR measurements in order to construct a continuous sedimentary sequence, and (3) discuss changes in the NGR signal in the time domain. This attempt gives us preliminary information to discuss climate stability in relation to orbital forcing thorough geologic time. NGR values are obtained mainly by indirectly measuring the amount of terrigenous minerals including potassium and related elements in the sediments. NGR intensity is also affected by high porosity, which in these sediments was related to the amount of diatom valves. NGR signals might be a proxy of the intensity of the East Asian monsoon off Sanriku. A continuous sedimentary record was constructed by integra-

¹Sakamoto, T., Saito, S., Shimada, C., and Yamane, M., 2003. Core-log integration of natural gamma ray intensity to construct a 10-m.y. continuous sedimentary record off Sanriku, western Pacific margin, ODP Sites 1150 and 1151. In Suyehiro, K., Sacks, I.S., Acton, G.D., and Oda, M. (Eds.), *Proc. ODP, Sci. Results*, 186, 1-42 [Online]. Available from World Wide Web: <http://www-odp.tamu.edu/publications/186_SR/VOLUME/CHAPTERS/112.PDF>. [Cited YYYY-MM-DD]

²Institute for Frontier Research on Earth Evolution (IFREE), Japan Marine Science and Technology Center, 2-15 Natsushima-cho, Yokosuka 237-0061, Japan. tats-ron@jamstec.go.jp

³Deep Sea Research Department, Japan Marine Science and Technology Center, 2-15 Natsushima-cho, Yokosuka 237-0061, Japan.

⁴JSPS Research Fellow, Department of Geology, National Science Museum, 3-23-1 Hyakunin-cho, Shinjuku-ku, Tokyo 169-0073, Japan.

⁵JSPS Research Fellow, Ocean Research Institute, The University of Tokyo, 1-15-1 Minamidai, Nakano-ku, Tokyo 164-8639, Japan.

tion of the whole-core NGR intensity measured in sediments obtained from the drilled holes with that measured directly in the borehole by wireline logging, then using a stratigraphic age model to convert to a time series covering 1.3–9.7 Ma with a short break at ~5 Ma. High sedimentation rate (H) stages were identified in the sequence, related to intervals of low-amplitude precession and eccentricity variations. The transition of the dominant periodicities through the four H stages may correlate to major shifts in the climate system, including the onset of major Northern Hemisphere glaciation, the initial stage of the East Asian monsoon intensification, and the onset of the East Asian monsoon with uplift of the Himalayas and the Tibetan Plateau.

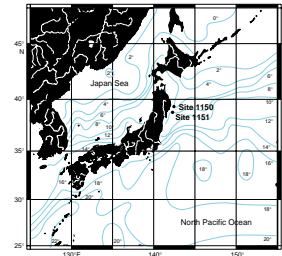
INTRODUCTION

Evolutionary processes of the Earth are recorded in the sediments and sedimentary rocks. Changes in the surface environment are reflected in features such as structure, thickness, grain size, and composition of stratigraphic sequences. If the stratigraphic sequence shows rhythmic or cyclic stratification or bedding, we call that “sedimentary rhythm.” By analyzing sedimentary rhythms in continuous sequences, we can reconstruct and attempt to understand paleoenvironmental changes (Merriam, 1964; Duff et al., 1967; Schwarzacher, 1975; Eincale and Seilacher, 1982; Berger et al., 1984; Hilgen, 1991; Lourens et al., 1996; Emeis et al., 2000).

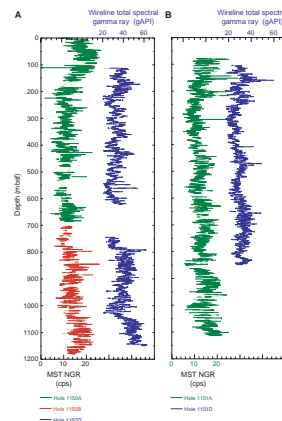
Climate response to orbital forcing has varied with geological time (e.g. Berger et al., 1984). For instance, prior to the Mid-Pleistocene Revolution (MPR), a period during the mid-Pleistocene when 100-k.y. periodicity of glacial-interglacial cycles intensified (Berger and Jansen, 1994), it is thought that the obliquity-band (41-k.y.) climatic periodicity was dominant in the Earth’s climate system (Maslin et al., 2001). The 41-k.y. obliquity cycles are the least common cycles evident since the onset of Northern Hemisphere glaciation (Imbrie et al., 1992). Although the amplitude and periodicity of the orbital parameters of the Earth, eccentricity (~100 k.y.), obliquity (~41 k.y.), and precession (~21 k.y.), did not change significantly during the MPR, glacial-interglacial cycles have shifted to 100 k.y. since the MPR. Imbrie et al. (1993) called this phenomenon the “100 ka problem” (Maslin et al., 2001). Because we can recognize only the last eight 100-k.y. cycles since the MPR, one way to discuss the stability of the climate system is to reveal the same climatic shift in older sedimentary records, such as during the late Miocene, when orbital parameters can be interpolated into the past (Laskar et al., 1993). A continuous sedimentary record is necessary to accomplish this objective.

During Ocean Drilling Program (ODP) Leg 186, we observed cyclic variations in whole-core multisensor track (MST) data from recovered cores and in wireline logging data sets at Sites 1150 and 1151, off Sanriku, northwestern Pacific margin (Figs. F1, F2). Data from nondestructive measurements, such as color reflectance, gamma ray attenuation (GRA) density, magnetic susceptibility, and natural gamma ray (NGR) intensity, for the recovered cores were synchronized at the meter scale, representing rhythmic sedimentary patterns (e.g., figs. F16 and F17 in Sacks, Suyehiro, Acton, et al., 2000). The coupled variations recognized in different parameters suggest underlying climatic and/or oceanographic variation.

F1. Locations of ODP sites, p. 13.



F2. NGR measured by wireline logging and MST, p. 14.



NGR is one useful lithologic parameter because clay mineral abundances can be estimated from NGR values, which are measurements of K, U, and Th. The clay mineral content in marine sediments provides important information concerning paleoceanographic variations such as terrigenous input and/or dilution by increased marine phytoplankton production. In this study, we report a series of physical, chemical, and paleontological data sets in relation to observed cyclic variations of whole-core MST NGR values in Leg 186 cores, in an attempt to identify source components of the NGR in the recovered cores and to construct a continuous 10-m.y. sedimentary record by integrating MST NGR data with wireline NGR data. Before using NGR signal as a paleoceanographic proxy, however, it is necessary to determine which parameters of chemical composition and/or physical properties relate to the NGR signal in a particular region. Downhole logging measurements provide high-resolution data for reconstruction of paleoceanographic history if core recovery was poor in the sequence. Core-log integration of physical properties such as NGR should give us a way to reconstruct a continuous sedimentary signal and a window to discuss the stability of our climate system in geological time.

MATERIALS AND METHODS

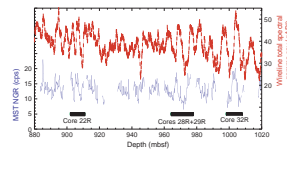
The thickness of the sedimentary sections recovered from Sites 1150 and 1151 were 1181.6 and 1113 m, respectively. These middle Miocene to Holocene sediments were obtained using the advanced piston corer (APC), extended core barrel (XCB), and rotary core barrel (RCB) coring systems (Sacks, Suyehiro, Acton, et al., 2000). RCB coring recovery averaged ~59% and 68%, respectively, for Sites 1150 and 1151. The section down to about 950 meters below seafloor (mbsf) at Site 1151 can be correlated with that at Site 1150, although the section at each site has a slightly different degree of lithification and physical properties differ. The major lithology of the recovered sediments predominantly consists of homogenous diatomaceous silty clay and diatomaceous clay and its lithified equivalents, which are variable admixtures mainly of biogenic siliceous microfossils, siliciclastic grains, and rare volcaniclastic grains (Sacks, Suyehiro, Acton, et al., 2000).

Five intervals in Cores 186-1150B-22R, 28R, 29R, and 32R and 186-1151A-91R and 105R were selected for detailed core-log integration. Clear cyclic variations were recognized in the MST data for recovered cores (Fig. F3). The purpose of this comparison is to identify the major factors that determine the NGR signal in the sedimentary sections. Samples were taken at ~20-cm intervals for Site 1150 and ~10-cm intervals for Site 1151, depending on sedimentation rate. Physical properties and major elements in bulk samples were analyzed. Diatom valve numbers and total organic carbon content were analyzed for selected samples.

MST and Wireline NGR

Individual whole-round core sections from Holes 1150B and 1151A were scanned on board the ship using the MST for magnetic susceptibility, GRA bulk density, *P*-wave velocity, and NGR emissions at constant intervals from the top to bottom depth of the section (Sacks, Suyehiro, Acton, et al., 2000). NGR intensity was measured at 20-cm intervals in each section with a sampling period of 20 s (Fig. F2). Data from 2048

F3. Correlation between wireline and MST NGR, p. 15.



energy channels were collected and archived, and counts were summed over the range from 200 to 3000 keV. This integration range allows comparison of the NGR data trends with those from downhole logging data, although the two methods measure NGR in different units (counts per second [cps] for the MST vs. gAPI [American Petroleum Institute gamma units] for downhole logging). The axial resolution on the MST is ~12 cm because of the geometry of the device, and the error of the system (estimated from reference values) varies from 3% to 7% (Blum, 1997). The MST reports NGR in counts per second because corrections for sampling volume are not made on shipboard measurements.

In situ wireline NGR measurements were collected using the Hostile Environment Natural Gamma Ray Sonde (HNGS) in Holes 1150D and 1151D (Fig. F2) (Sacks, Suyehiro, Acton, et al., 2000). The HNGS uses two bismuth germanate scintillation detectors for significantly improved tool precision to determine concentrations of K, Th, and U, the three elements whose isotopes dominate the natural radiation spectrum. Spectral analysis in the HNGS filters out gamma ray energies below 500 keV, eliminating sensitivity to bentonite or KCl in the drilling mud and improving measurement accuracy. The HNGS data were corrected for logging hole size during recording. The log responds to mineral composition and therefore indicates changes in lithology. The total spectral gamma ray value, which is the sum of the natural gamma ray intensities of the three elements, shows regular oscillations at ~5-m intervals in the middle part of the hole and at ~10-m intervals in the lower part of the section (Figs. F2, F3).

Major Elements

Major elements for bulk samples were measured using the energy-dispersive X-ray fluorescence analyzer (JOEL-JSX3211) (Table T1). Measurements were performed on dried, powdered, and tablet-pressed samples at operation parameters of 30.0 kV, 0.4 mA, and 600 s in a vacuum sample chamber. Element contents were quantified by fundamental parameter methods as oxides. Relative measurement error for each mineral was calculated as follows: Na₂O = 3.69 wt%; MgO = 0.7 wt%; Al₂O₃ = 0.4 wt%; SiO₂ = 0.2 wt%; K₂O = 1.39 wt%; CaO = 0.70 wt%; TiO₂ = 1.79 wt%; MnO = 1.35 wt%; and Fe₂O₃ = 0.10 wt%, by duplicate measurement for a series of standard samples from the Geological Survey of Japan (JA-2, JB-1b, JG-1a, JGb-1, JH-1, JR-3, JMn-1, JCh-1, JD0-1, JLs-1, JLk-1, JSd-1, JSd-2, and JSd-3).

T1. Major element analysis, p. 26.

Physical Properties

Samples of ~10 cm³ were used to determine laboratory-based precise physical properties (Table T2). Measurements of the wet and dry mass and the dry volume of a sample were used to determine the moisture and density using the same procedure as that used during the cruise (i.e., Method C of Blum, 1997). Sample mass was determined with an error within ±0.1%, which was counterbalanced by a known mass such that the mass differentials were less than ~5 g. Bulk dry weight and volume measurements were performed after the samples were oven dried at 105 ± 5°C for 24 hr and allowed to cool in a desiccator. Grain density of samples was determined using a Quantachrome pentapycnometer, a helium-displacement pycnometer. The density was determined at least

T2. Physical properties, p. 31.

five times with <0.01% standard deviation. This exercise demonstrated that the measured grain density had a precision of about $\pm 0.01 \text{ g/cm}^3$.

Water content (based on total wet mass and mass of solids), dry bulk density, grain density, and porosity were calculated from the measured data using the following equations. Assumptions and relationships of moisture and density properties were corrected for salinity and density of the pore water following Boyce (1976). The determination of water content followed the methods of the American Society for Testing and Materials (ASTM) designation (D) 2216 (ASTM, 1989). In situ shipboard measurements of the salinity of pore water showed that it was significantly lower than the standard salinity used for automatic calculations (0.035). Therefore, moisture and density were recalculated using in situ values of salinity and density of the pore water. The pore water density is a function of temperature, salinity, and pressure (Blum, 1997). At laboratory temperature and pressure conditions ($T = 20^\circ\text{C}$; $P = 1 \text{ bar}$), we derived the following relationship between density (ρ_{pw}) and salinity (s) of pore water by fitting the data to a line (see fig. 2-1 of Blum, 1997):

$$\rho_w = 0.998 + 7.7143 \times s. \quad (1)$$

To allow cross-examination of the data for internal consistency, values of porosity, dry density, and void ratio were calculated indirectly from the other moisture and density properties:

$$\phi = 100 \times [(\rho_g/1.024 - \rho_b)/(\rho_g/1.024 - \rho_{pw})]; \quad (2)$$

$$\phi = W_s \times \rho_b / [(1 + W_s/100) \times \rho_{pw}]; \quad (3)$$

$$\rho_d = \rho_{pw} \times \phi/W_s; \text{ and} \quad (4)$$

$$e = \rho_g \times W_s / (\rho_{pw} \times 100). \quad (5)$$

where,

- ϕ = porosity,
- ρ_g = grain density,
- ρ_b = bulk density,
- ρ_{pw} = pore water density,
- W_s = water content,
- ρ_d = dry density, and
- e = void ratio.

Diatom Abundances and Total Organic Carbon

Samples from Cores 186-1150B-22R, 28R, 29R, and 32R were analyzed for diatom abundances and total organic carbon to evaluate the contribution of biogenic components to the bulk chemical composition (Table T3). Samples for diatom analysis (20 mg) were processed by treating them with 10% hydrogen peroxide to remove organic material and with 10% hydrochloric acid to remove carbonate after drying. The samples were subsequently diluted with 50 mL of distilled water to remove the chemical solutions from the suspension. Suspensions of 0.5 mL were pipetted and dried on 18-mm-diameter coverslips and completed as smear slides to be examined at a magnification of 1250 \times with a microscope. The slides were examined in their entirety to count num-

T3. Diatom and TOC analyses,
p. 37.

bers of total diatom valves. The number of valves was converted to an absolute number per gram of sample.

Dried samples for total organic carbon (TOC) analyses were powdered using an agate mortar. Carbonate was removed with 2-N HCl after drying and weighing, and TOC was analyzed using a Fisons CHN elemental analyzer (NA-1500). Precision of measurement is better than ± 0.01 wt%.

RESULTS AND DISCUSSION

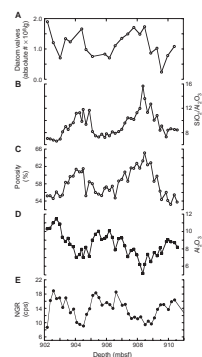
NGR Intensity Sources

NGR is a useful lithologic parameter because the primeval emitters are at secular equilibrium (i.e., radiation at characteristic energies is constant with time) (Adams and Gasparini, 1970; Blum, 1997). Radioisotopes with sufficiently long life and that decay to produce an appreciable amount of gamma rays are potassium (^{40}K) with a half-life of 1.3×10^9 yr, thorium (^{232}Th) with a half-life of 1.4×10^{10} yr, and uranium (^{238}U) with a half-life of 4.4×10^9 yr. The total NGR intensity is a function of the combined contributions of K, U, and Th in sediments, matrix density, and matrix lithology. Matrix density mainly results from Compton scattering, and matrix lithology results from photoelectric absorption (Blum, 1997). Clay mineral content is often diluted by other components such as biogenic silica. Because of this dilution, if the NGR signal in the sedimentary sequence is to be used to reconstruct the environmental record, it is important to know which chemical components really relate to the NGR signal.

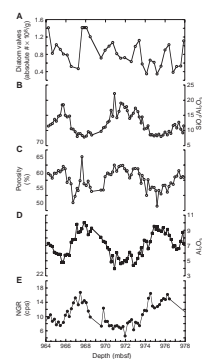
The NGR intensity of sediments from Cores 186-1150B-22R, 28R, 29R, and 32R and 186-1151A-91R and 105R are plotted with analyzed chemical results in Figures F4, F5, F6, F7, and F8. NGR intensity shows cyclic behavior in these intervals. Cyclic variation corresponding to that of NGR intensity was observed in a series of properties in recovered sediments. Major elements in bulk samples were Na_2O , MgO , Al_2O_3 , SiO_2 , S, K_2O , CaO , TiO_2 , MnO , and Fe_2O_3 (Table T1). SiO_2 is the most abundant element off Sanriku (76.3 wt% on average of all samples) and is more abundant at northern Site 1150 (79.0 wt%) than at Site 1151 (72.2 wt%). In contrast, Al_2O_3 , which is the second most abundant element, is 9.5 wt% on average at Site 1151, compared to 7.4 wt% at Site 1150. MgO , K_2O , TiO_2 , and Fe_2O_3 have positive correlations with Al_2O_3 content, which is slightly richer at Site 1151 than at Site 1150, which included siliciclastic minerals. NGR correlates positively with Al_2O_3 and K_2O at Site 1150 (Fig. F9A, F9B). Although this relationship is not clear at Site 1151, NGR intensity and Al_2O_3 and K_2O contents are higher than at Site 1150. The amount of terrigenous minerals including K, Al, and related elements such as clay minerals are the principal sources of the NGR intensity.

Terrigenous components are often diluted by other components such as biogenic components. The sediments consist mainly of biogenic and terrigenous components with small amounts of volcaniclastic particles off Sanriku (Sacks, Suyehiro, Acton, et al., 2000). In turn, SiO_2 contents in hemipelagic marine sediments consist of both biogenic and detrital SiO_2 with small amounts of volcanogenic silica. Off Sanriku, biogenic silica, especially diatom valves, is a major component of biogenic particles. A plot of SiO_2 vs. Al_2O_3 contents shows wide scattering across the

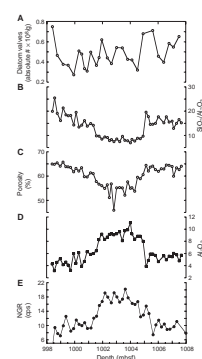
F4. Core 186-1150B-22R properties, p. 16.



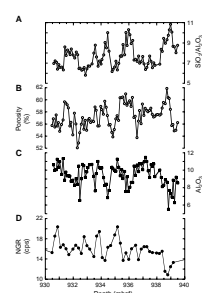
F5. Cores 186-1150B-28R and 29R properties, p. 17.



F6. Core 186-1150B-32R properties, p. 18.



F7. Core 186-1151A-91R properties, p. 19.



full data range, with a linear negative slope line on the upper limit of their ranges (Fig. F9C). The linear negative slope line means that there is a dilution relationship between biogenic silica and terrigenous aluminum. Other silica on the straight lines, which pass through the origin of the coordinates in Figure F11C, shows terrigenous silica included in siliciclastic minerals. The relation of biogenic and detrital silica is much clearer in Figure F9D. The $\text{SiO}_2/\text{Al}_2\text{O}_3$ ratio has a clear negative correlation with Al_2O_3 content (Fig. F9D). The samples with high $\text{SiO}_2/\text{Al}_2\text{O}_3$ ratios, representing high biogenic silica, correspond to those with high TOC (Fig. F9E). TOC off Sanriku should mainly derive from sea-surface production of siliceous phytoplankton dominated by diatoms. The $\text{SiO}_2/\text{Al}_2\text{O}_3$ ratio is weakly correlated with the number of diatom valves (Fig. F9F). Because the counting methods for diatom valves under the microscope may not be quantitative, the relationship may not be clear.

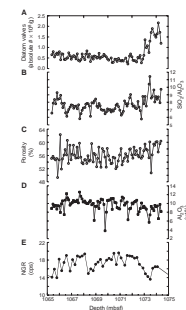
Pore volume and/or density may have some control on the NGR signal if downcore variations in NGR activity are low (Blum, 1997). Porosity variations are proportional to the concentration of the matrix in sediments, which may be proportional to the concentration of a radioactive mineral in the sediments. This implies that NGR intensity is a reflection of compositional control of terrigenous minerals including radioactive elements and biogenic silica (Fig. F10A). The high NGR intensity (10–20 cps) shows negative correlation with the $\text{SiO}_2/\text{Al}_2\text{O}_3$ ratio of weight percent, which ranges between 5 and 15 (Fig. F10A). In addition, there is an excess value of the ratio above the linear negative slope line at ~10 cps of NGR intensity. The NGR intensity has negative correlation with porosity at Site 1150 (Fig. F10B). The correlation at Site 1151 is not as obvious as that at Site 1150 but shows weak negative correlation. Grain density, however, does not vary with the NGR intensity (Fig. F11D). Therefore, the NGR intensity is affected by the compositional changes of diatom-dominant biogenic silica and terrigenous particles dominated by clay minerals. High porosity values corresponding to the high the excess value of the $\text{SiO}_2/\text{Al}_2\text{O}_3$ ratio correlates to low NGR intensity. The porous structure of diatom valves results in high porosity of bulk sediments.

Consequently, the NGR intensity off Sanriku is controlled mainly by composition of terrigenous minerals with biogenic silica dilution. It was also affected by high porosity related to the amount of diatom valves. Using the analogy that the East Asian monsoon has a great influence on land precipitation and marine productivity in the present day, the NGR signal might to be a proxy of the past intensity of the East Asian monsoon off Sanriku.

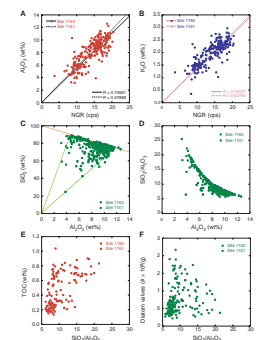
Core-Log Integration of NGR Intensity

In order to construct a continuous sedimentary record and to estimate stratigraphic ages in the logged hole to correlate with ages identified in the recovered cores, it is necessary to integrate the whole-core MST NGR intensity from Holes 1150A and 1150B with the wireline logging NGR intensity in Hole 1150D. As there was a depth shift between depth of recovered core and that of the borehole logs (e.g., Fig. F2), a procedure was necessary to compensate for the depth shift between the holes before core-log integration of NGR intensity. NGR measurements using the HNGS were reported at the most precise depths (Sacks, Suyehiro, Acton, et al., 2000). In this study, the depths of recovered cores were adjusted to the downhole logging depth by graphically correlating

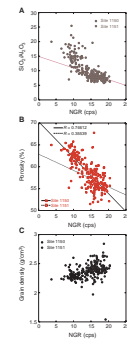
F8. Core 186-1151A-105R properties, p. 20.



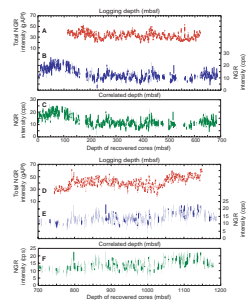
F9. Relationships between properties at Sites 1150 and 1151, p. 21.



F10. Relationships between NGR and other properties, p. 22.



F11. Depth shift between MST and wireline NGR, p. 23.



obvious peaks and troughs in the NGR profile Site 1150 (Table T4). Variations of the NGR profile in MST and logging data are illustrated in Figure F11. Recovered core depths between the top of the core and 117.7 mbsf, between 700 and 729 mbsf, and below 1146 mbsf shifted linearly –3.3 m, –1.9 m, and –1.1 m, respectively. Logging depths are known to be accurate above 117.7 mbsf because the end of pipe was set at about that depth. NGR was not logged between 700 and 729 mbsf or below 1146 mbsf (Table T4). The depth offset between Holes 1150A and 1150D ranged from +0.9 to –7.6 m (average = –2.4 m) and that between Holes 1150B and 1150D ranged from +1.3 to –7.0 m (average = –1.4 m) (Table T4). Although the logging NGR units (gAPI) are different from the MST NGR units (cps), the trends between core and log NGR can be compared after depth adjustment.

Variations of NGR Intensity though Time

The logging NGR intensity was converted to a time series using a stratigraphic age model. Depths of stratigraphic events in Holes 1150A and 1150B were correlated to Hole 1150D in this procedure. The age model for Site 1150 used in this study is based on biostratigraphy and magnetostratigraphy for Holes 1150A and 1150B (Table T5). Biostratigraphic datums were based on Maruyama and Shiono (this volume), Kamikuri et al. [N1], and Li (this volume). Magnetochronology was based on Leg 186 shipboard stratigraphy (Sacks, Suyehiro, Acton, et al., 2000). In this study, only stratigraphic events that could determine ultimate age were used (Table T5); events that could determine age in some intervals were left out. Middepths of the events were used in the transferring procedure, if stratigraphic events were identified in intervals. As a result, the sedimentary sequence from 1.3 to 9.7 Ma was constructed with a short break at ~5 Ma (Fig. F12).

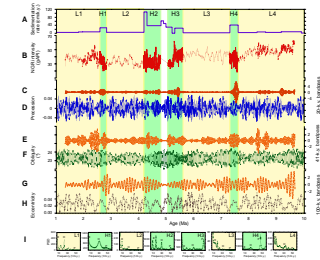
Based on linear sedimentation rates, which were calculated for the intervals between the stratigraphic events, eight stages of low (L) and high (H) sedimentation rate were identified (Fig. F12A; Table T6). Average sedimentation rates ranged from 3 to 10 cm/k.y. in L stages and from 19 to 73 cm/k.y. in H stages. NGR data were bandpass filtered at 100, 41, and 20 k.y. after resampling the original data in order to equalize sampling intervals to uniform rates (Fig. F12C, F12E, F12G; Table T6). The bandpass filter was centered at a period of 100 k.y. between 83 and 125 ka, 41 k.y. between 35 and 49 ka, and 21 k.y. between 19 and 24 ka. The power spectrum density (PSD) of the maximum entropy method (MEM) for each stage was calculated for the modified time series of the NGR variation between 2 and 100 (1/m.y.) frequency. A numerical series procedure was performed using the software program developed by Paillard et al. (1996). Depending on time control points (average interval = 0.442 m.y.), detailed discussion for values of periodicities was not possible, but the eccentricity, obliquity, and precession band periodicities were detected (Fig. F12I).

The H stages, especially H1, H2, and H4, corresponded to the intervals of low-amplitude precession index and eccentricity calculated by Laskar (1993) (Fig. F12D, F12H), therefore high sedimentation rates in the stages might not be always artificial. During the H stages, the power of the precession band component in the NGR signal was high, particularly in the H4 stage. Obliquity band and eccentricity band components always existed through 10 Ma. The obliquity band periodicities had high power in the L1 stage and moderate power in L4 stage. The power of those became weak in the L stages before the H1, H3, and H4 stages.

T4. Splice tie points and depth offsets, p. 39.

T5. Stratigraphic events used for correlation, p. 40.

F12. NGR with orbital parameters, p. 24.



T6. Low and high sedimentation rate stages, p. 41.

Intensity changes in the periodic components in each stage through time suggest that the climate system reorganized during the H stages, particularly the H1 and H4 stages. An eccentricity-dominant system with moderate precession and obliquity in the L4 stage seemed to switch an eccentricity-dominant system with low precession and obliquity in the L3 through H4 stages. An eccentricity-dominant system with low precession and obliquity in the L2 stage seemed to switch to an obliquity-dominant system with low precession in the L1 through H1 stages. Transition of the dominant periodicities during the H stages may correspond to major shifts in the climate system. The H1 stage could be correlated with the onset of the East Asian monsoon, which is linked with the uplift of the Himalayas and the Tibetan Plateau. The uplift could have reached sufficient height at that time to produce rainfall in the Asian continental margin, causing increasing river runoff and transporting terrigenous minerals from land into the northwest Pacific. The L2 and L3 stages might indicate the initial stage of the East Asian monsoon intensification through the H2 and H3 stages. The H4 stage could correspond to the strengthening/transitional stage of the monsoon system at ~3.0–2.6 Ma. The timing matches the onset of major Northern Hemisphere glaciation. The L1 stage has been the prevailing stage of the monsoon since 2.7 Ma, relating to Quaternary climatic fluctuations on an glacial-interglacial timescale after the onset of major Northern Hemisphere glaciation.

SUMMARY AND CONCLUSIONS

In this study, we reported the coupled variations recognized in chemical composition and physical properties in the drilled and logged holes at Sites 1150 and 1151. NGR intensity was one useful parameter for reconstruction of paleoceanographic changes. The analytical results showed that (1) the amount of terrigenous minerals including K, Al, and related elements such as clay minerals were the principal sources of the NGR intensity, (2) the NGR intensity was also affected by high porosity related to the amount of diatom-dominant biogenic silica, and (3) NGR signal might be a proxy for the intensification of the East Asian monsoon off Sanriku.

A continuous sedimentary record was constructed by integration of the whole-core MST NGR intensity from Holes 1150A and 1150B with the wireline NGR log from Hole 1150D. Using a stratigraphic age model, the constructed sedimentary sequence was converted to a time series sequence from 1.3 to 9.7 Ma with a short break at ~5 Ma. The results obtained indicate that

1. The sequence can be divided into eight stages of low (L) and high (H) sedimentation.
2. The H stages correspond to the low-amplitude intervals of precession index and eccentricity.
3. Power spectral density of the precession band component in the NGR signal was high during the H stages.
4. Obliquity band and eccentricity band components always existed through 10 Ma.
5. Changes of intensities of the periodic components through time suggested that the climate system reorganized during the H stages.
6. Transition of the dominant periodicities during the H stages may correspond to major shifts of the climate system. The H1, H2/

H3, and H4 stages could be correlated to the onset of major Northern Hemisphere glaciation, the initial stage of the East Asian monsoon intensification, and onset of the East Asian monsoon with uplift of the Himalayas and the Tibetan Plateau, respectively.

This is the first attempt at core-log integration of NGR intensity in an attempt to identify the sources of NGR off Sanriku. It is still necessary to determine the detailed paleoceanographic setting for variations in terrigenous input and marine productivity of diatoms. In addition, because of the uncertainty of time control points, future precise work is necessary to prove the prospective interpretations for the NGR variations in time.

ACKNOWLEDGMENTS

We thank the two co-chief scientists, shipboard scientists, technicians, and crew of the *JOIDES Resolution* of ODP Leg 186 and land-based staff at ODP, Texas A&M University, for their assistance and cooperation for this study. This research used samples and data provided by the Ocean Drilling Program (ODP). The ODP is sponsored by the U.S. National Science Foundation (NSF) and participating countries under management of Joint Oceanographic Institutions (JOI), Inc. T. Sakamoto thanks the Ministry of Education, Culture, Sports, Science and Technology for funding (grant no. 11740277). C. Shimada and M. Yamane were funded by the fellowship of the Japanese Society of the Promotion of Science (JSPS). We express our gratitude to two anonymous reviewers.

REFERENCES

- Adams, J.A.S., and Gasparini, P., 1970. Gamma ray spectrometry of rocks. In *Methods of Geochemistry and Geophysics 10*: Amsterdam (Elsevier).
- ASTM, 1989. *Annual Book of ASTM Standards for Soil and Rock: Building Stones* (Vol. 4.08): *Geotextiles*: Philadelphia (Am. Soc. Testing and Mater.).
- Berger, A., Imbrie, J., Hays, J., Kukla, G., and Saltzman, B. (Eds.), 1984. *Milankovitch and Climate* (Pts. 1 and 2): NATO ASI Ser., Ser. C, 126.
- Berger, W.H., and Jansen, E., 1994. Mid-Pleistocene climate shift: the Nansen connection. In Johannessen, O.M., Muensch, R.D., and Overland, J.E. (Eds.), *The Role of the Polar Oceans in Shaping the Global Environment*. Geophys. Monogr., Am. Geophys. Union, 85:295–311.
- Blum, P., 1997. Physical properties handbook: a guide to the shipboard measurement of physical properties of deep-sea cores. *ODP Tech. Note*, 26 [Online]. Available from World Wide Web: <<http://www-odp.tamu.edu/publications/tnotes/tn26/INDEX.HTM>>. [Cited 2002-01-02]
- Boyce, R.E., 1976. Definitions and laboratory techniques of compressional sound velocity parameters and wet-water content, wet-bulk density, and porosity parameters by gravimetric and gamma-ray attenuation techniques. In Schlanger, S.O., Jackson, E.D., et al., *Init. Repts. DSDP*, 33: Washington (U.S. Govt. Printing Office), 931–958.
- Duff, P.M., Hallam, A., and Walto, E.K. (Eds.), 1967. *Cyclic Sedimentation, Developments in Sedimentology 10*: Amsterdam (Elsevier).
- Einsele, G., and Seilacher, A. (Eds.), 1982. *Cycle and Event Stratification*: Berlin (Springer-Verlag).
- Emeis, K.-C., Sakamoto, T., Wehausen, R., and Brumsack, H.-J., 2000. The sapropel record of the eastern Mediterranean Sea—results of Ocean Drilling Program Leg 160. *Palaeogeogr., Palaeoclimatol., Palaeoecol.*, 158:259–280.
- Hilgen, F.J., 1991. Astronomical calibration of Gauss to Matuyama sapropels in the Mediterranean and implication for the geomagnetic polarity time scale. *Earth Planet. Sci. Lett.*, 104:226–244.
- Imbrie, J., Berger, A., Boyle, E., Clemens, S., Duffy, A., Howard, W., Kukla, G., Kutzbach, J., Martinson, D., McIntyre, A., Mix, A., Molfino, B., Morley, J., Peterson, L., Pisias, N., Prell, W., Raymo, M., Shackleton, N., and Toggweiler, J., 1993. On the structure and origin of major glaciation cycles, 2. The 100,000-year cycle. *Paleoceanography*, 8:699–735.
- Imbrie, J., Boyle, E.A., Clemens, S.C., Duffy, A., Howard, W.R., Kukla, G., Kutzbach, J., Martinson, D.G., McIntyre, A., Mix, A.C., Molfino, B., Morley, J.J., Peterson, L.C., Pisias, N.G., Prell, W.L., Raymo, M.E., Shackleton, N.J., and Toggweiler, J.R., 1992. On the structure and origin of major glaciation cycles, 1. Linear responses to Milankovitch forcing. *Paleoceanography*, 7:701–738.
- Laskar, J., Joutel, F., and Boudin, F., 1993. Orbital, precessional, and insolation quantities for the Earth from -20 Myr to +10 Myr. *Astron. Astrophys.*, 270:522–533.
- Lourens, L.J., Antonarakou, A., Hilgen, F.J., Van Hoof, A.A.M., Vergnaud-Grazzini, C., and Zachariasse, W.J., 1996. Evaluation of the Plio-Pleistocene astronomical timescale. *Paleoceanography*, 11:391–413.
- Maslin, M.A., Seidov, D., and Lowe, J., 2001. Synthesis of the nature and causes of rapid climate transitions during the Quaternary. In Seidov, D., Haupt, B.J., and Maslin, M.A. (Eds.), *The Oceans and Rapid Climate Change: Past, Present, and Future*. Geophys. Monogr., Am. Geophys. Union, 126:9–52.
- Merriam, D.F. (Ed.), 1964. *Symposium on Cyclic Sedimentation*. Bull.—Kans. Geol. Surv., 169.
- Paillard, D., Labeyrie, L., and Yiou, P., 1996. Macintosh program performs time-series analysis. *Eos*, 77:379.

- Sacks, I.S., Suyehiro, K., Acton, G.D., et al., 2000. *Proc. ODP, Init. Repts.*, 186 [CD-ROM]. Available from: Ocean Drilling Program, Texas A&M University, College Station TX 77845-9547, USA.
- Schwarzacher, W., 1975. *Sedimentation Models and Quantitative Stratigraphy*: Amsterdam (Elsevier), Dev. in Sedimentol. Ser., 19.

Figure F1. Locations of ODP Sites 1150 and 1151, off Sanriku in the northwestern Pacific margin. Annual average sea-surface temperatures are shown in degrees Celsius.

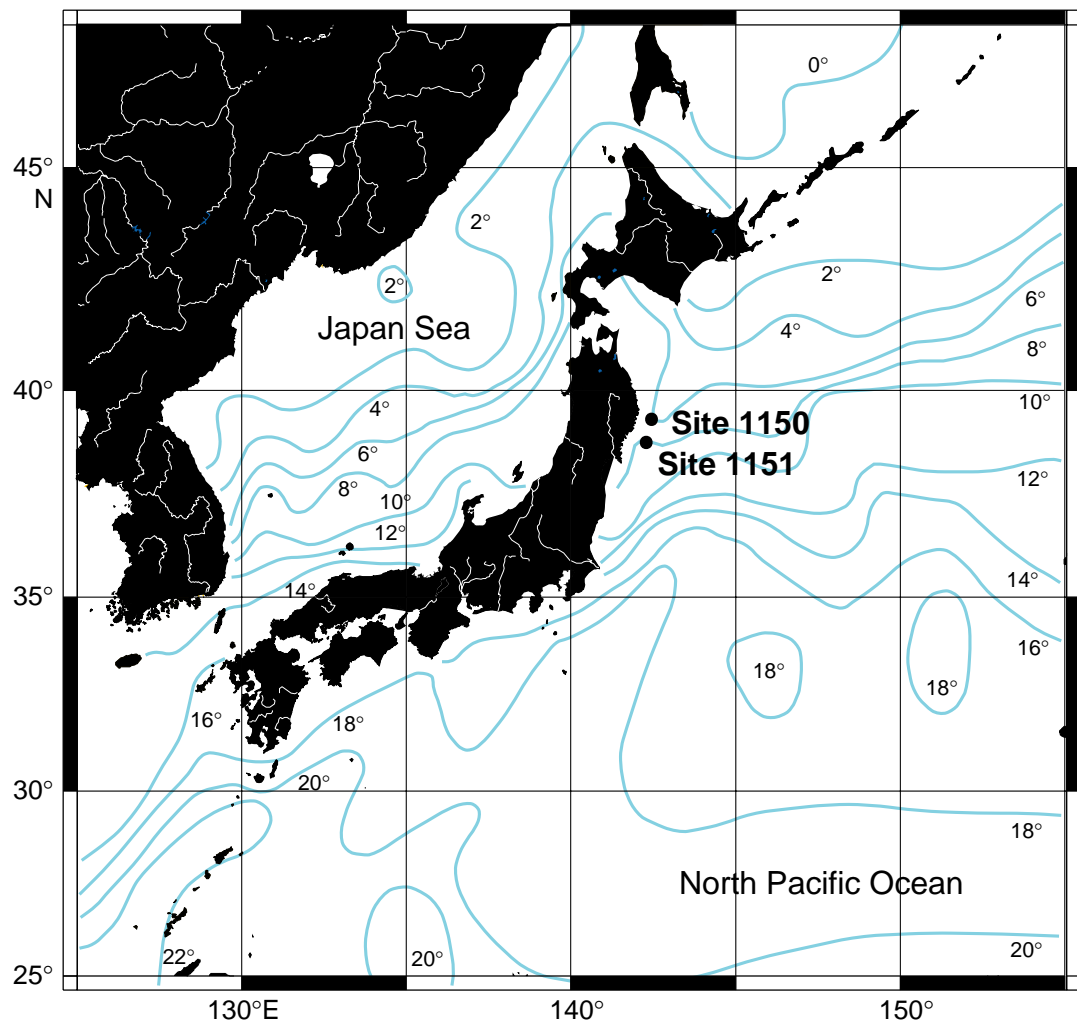


Figure F2. Variations of total spectral gamma ray intensity measured by wireline logging and natural gamma ray (NGR) intensity on whole cores measured on the multisensor track (MST) at (A) Site 1150 and (B) Site 1151.

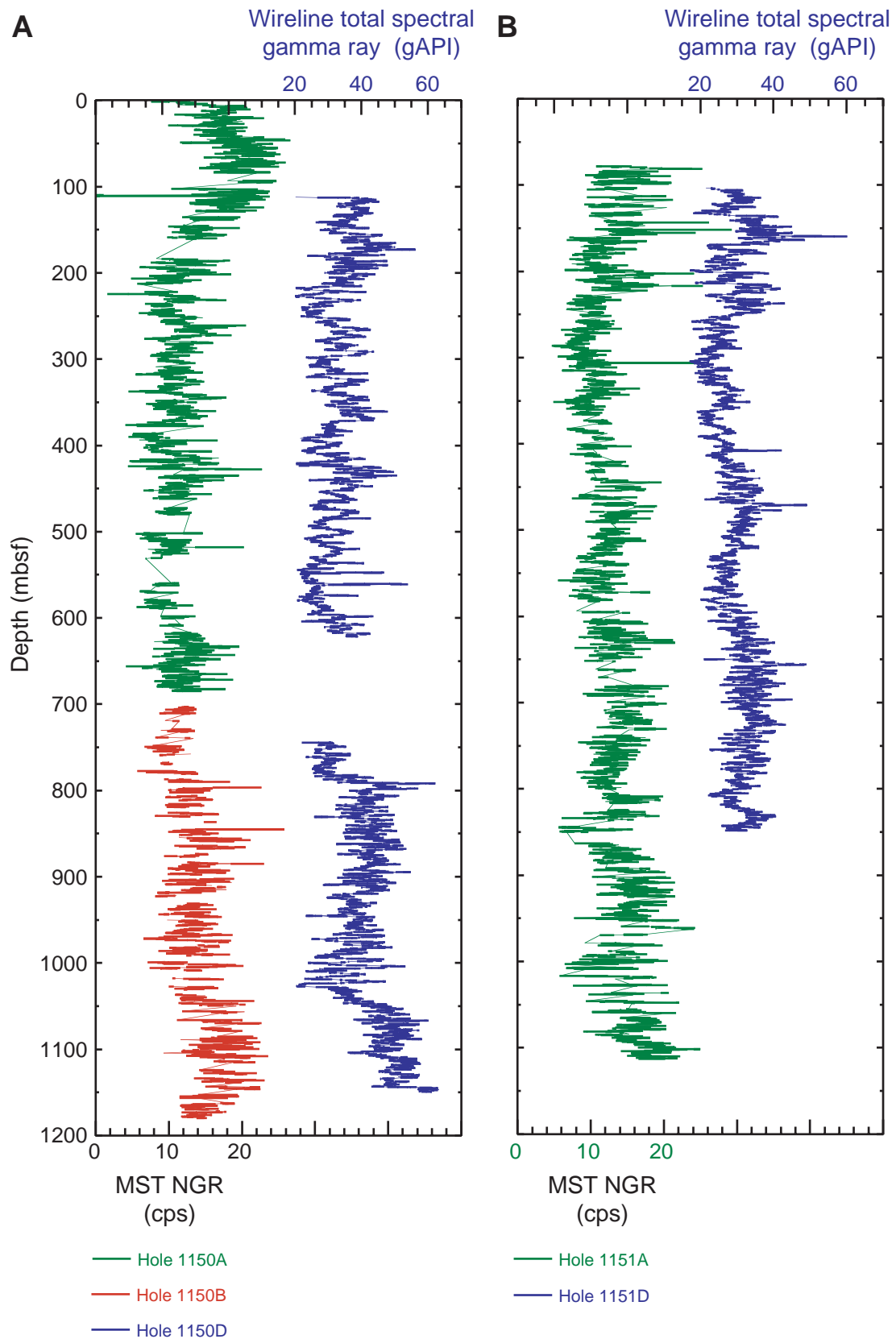


Figure F3. Correlation between total spectral gamma ray intensity measured by wireline logging in Hole 1150D and natural gamma ray (NGR) intensity of recovered cores in Hole 1150B. Intervals for Cores 186-1150B-22R, 28R + 29R, and 32R are shown as bars.

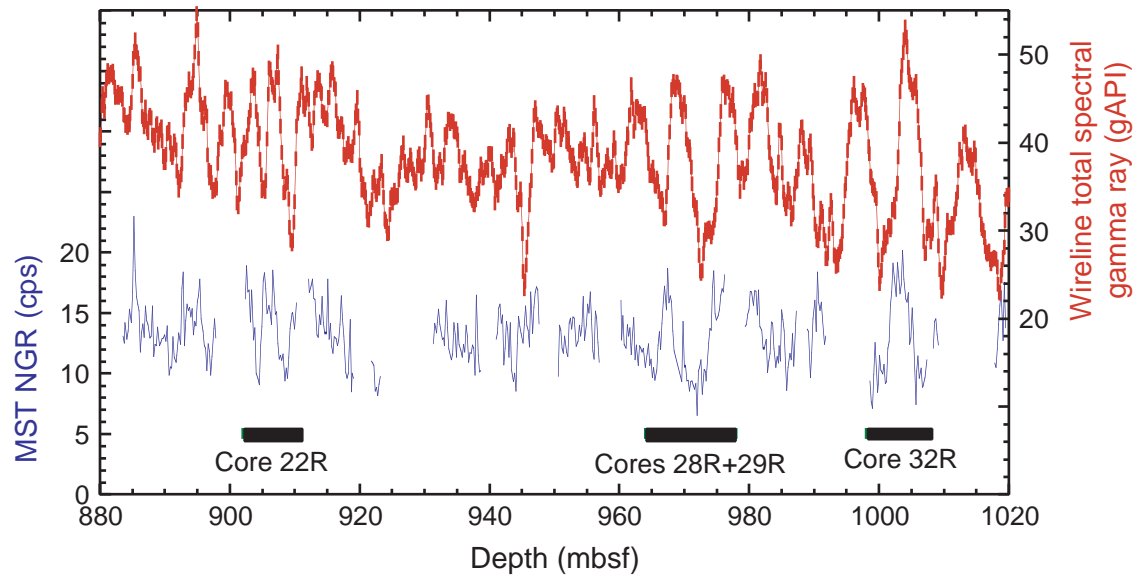


Figure F4. Cyclic variation of a series of properties in recovered sediments from Core 186-1150B-22R.
A. Absolute diatom valve numbers. **B.** $\text{SiO}_2/\text{Al}_2\text{O}_3$ ratio. **C.** Porosity. **D.** Al_2O_3 content. **E.** Natural gamma ray (NGR) intensity.

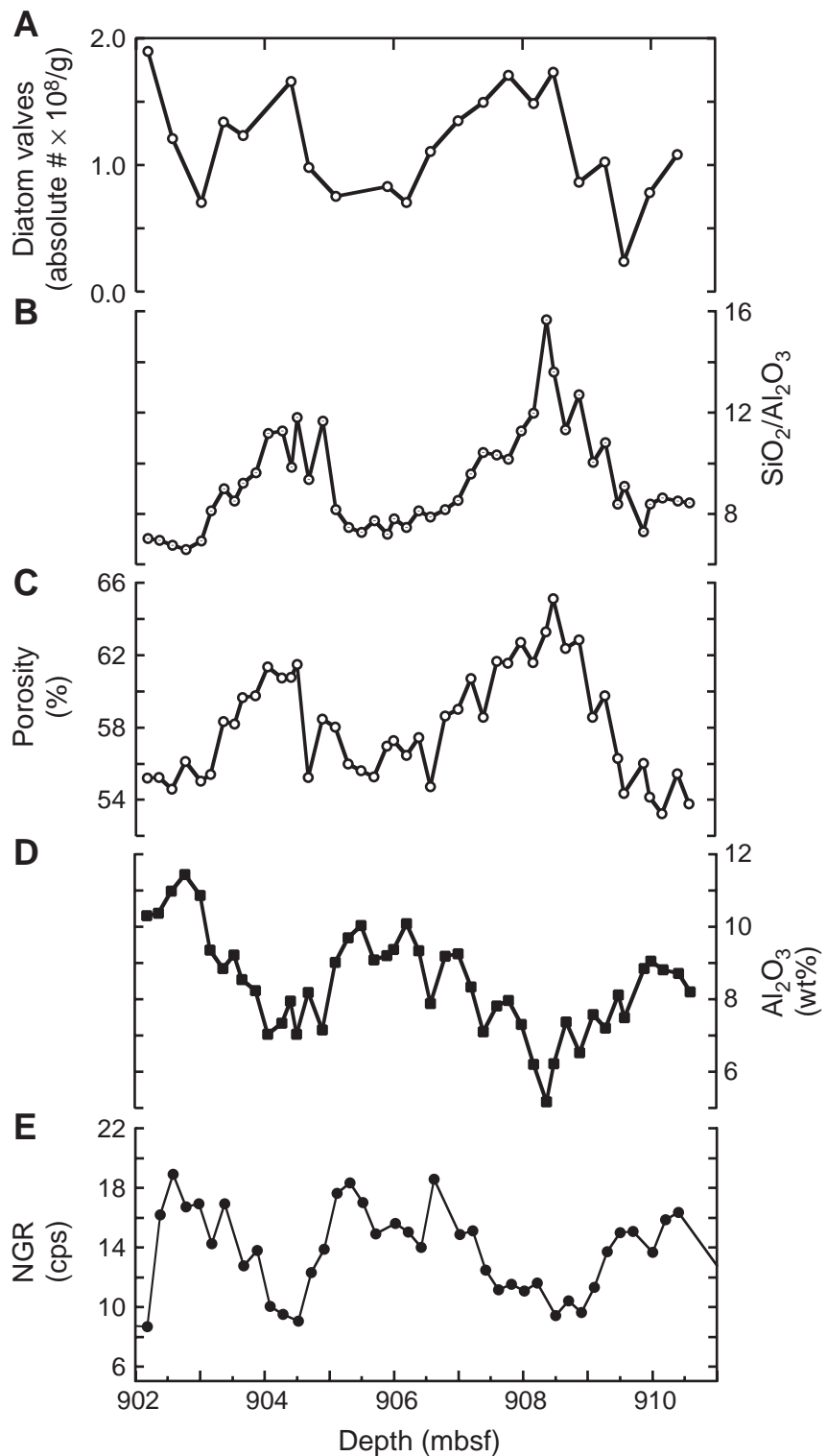


Figure F5. Cyclic variation of a series of properties in recovered sediments from Cores 186-1150B-28R and 29R. A. Absolute diatom valve numbers. B. $\text{SiO}_2/\text{Al}_2\text{O}_3$ ratio. C. Porosity. D. Al_2O_3 content. E. Natural gamma ray (NGR) intensity.

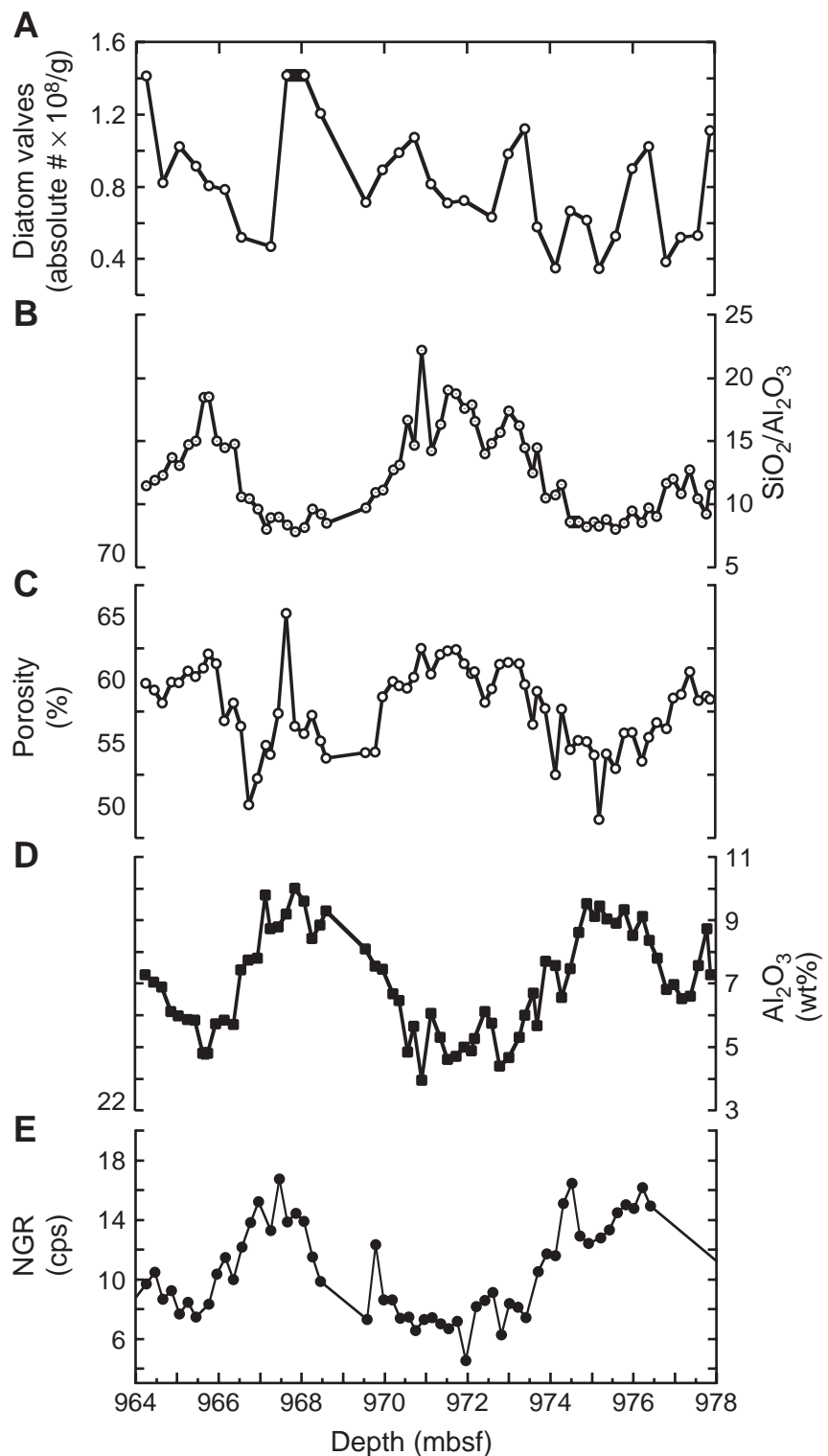


Figure F6. Cyclic variation of a series of properties in recovered sediments from Core 186-1150B-32R.
A. Absolute diatom valve numbers. **B.** $\text{SiO}_2/\text{Al}_2\text{O}_3$ ratio. **C.** Porosity. **D.** Al_2O_3 content. **E.** Natural gamma ray (NGR) intensity.

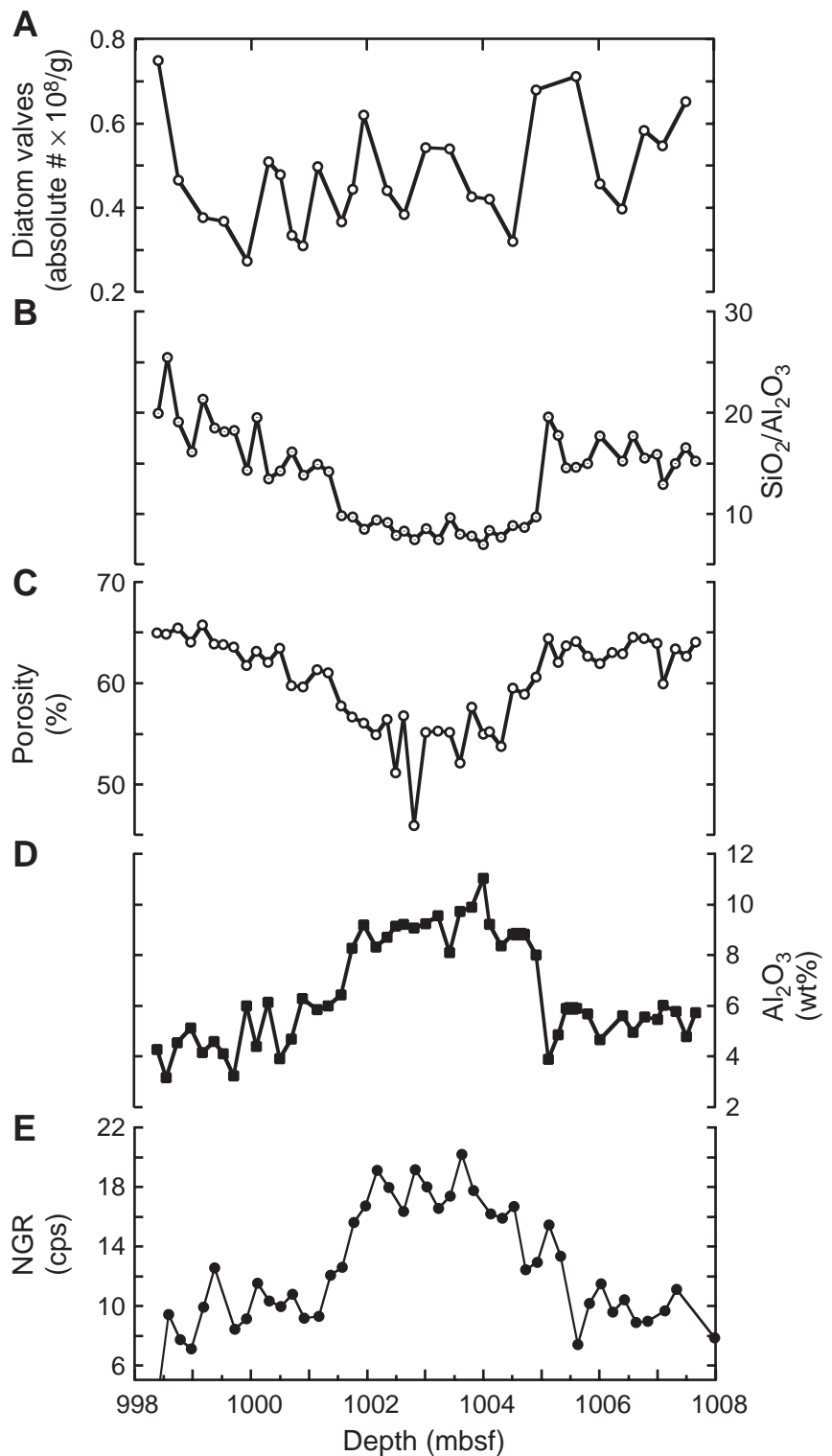


Figure F7. Cyclic variation of a series of properties in recovered sediments in Core 186-1151A-91R. A. $\text{SiO}_2/\text{Al}_2\text{O}_3$ ratio. B. Porosity. C. Al_2O_3 content. D. Natural gamma ray (NGR) intensity.

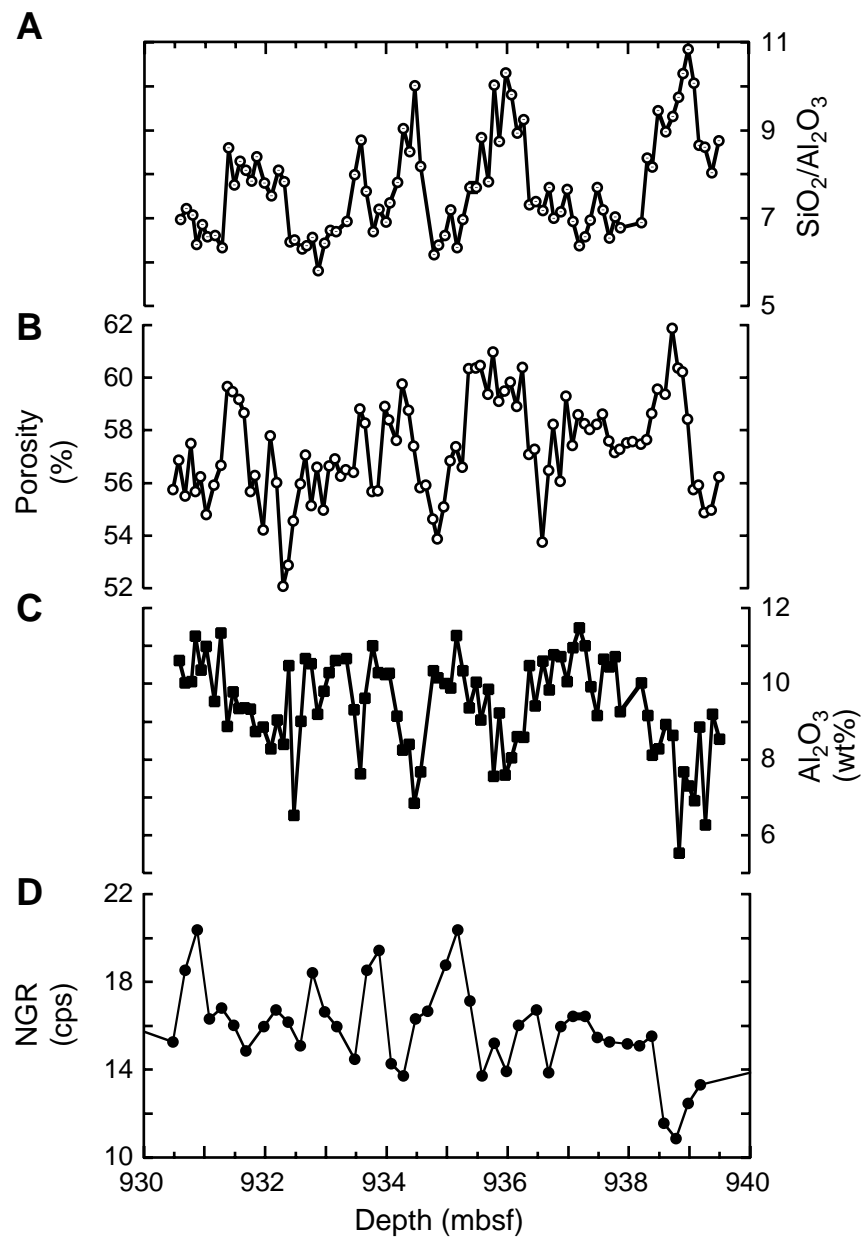


Figure F8. Cyclic variation of a series of properties in recovered sediments from Core 186-1151A-105R.
A. Absolute diatom valve numbers. **B.** $\text{SiO}_2/\text{Al}_2\text{O}_3$ ratio. **C.** Porosity. **D.** Al_2O_3 content. **E.** Natural gamma ray (NGR) intensity.

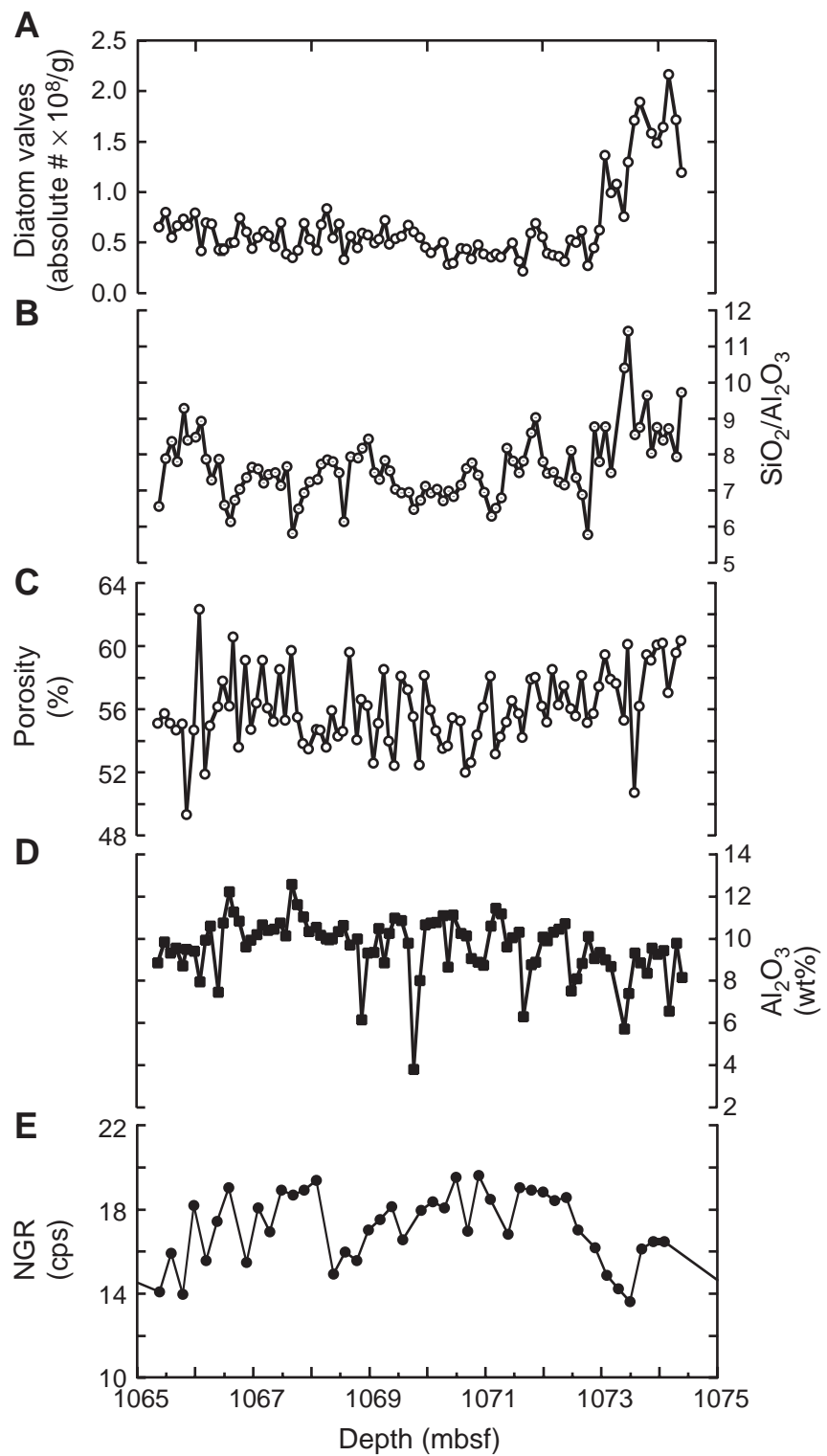


Figure F9. Relationships between properties at Sites 1150 and 1151. A. Natural gamma ray (NGR) intensity vs. Al_2O_3 . B. NGR vs. K_2O . C. Al_2O_3 vs. SiO_2 content. D. $\text{SiO}_2/\text{Al}_2\text{O}_3$ ratio vs. Al_2O_3 content. E. $\text{SiO}_2/\text{Al}_2\text{O}_3$ ratio vs. total organic carbon (TOC) content. F. $\text{SiO}_2/\text{Al}_2\text{O}_3$ ratio vs. diatom valve numbers.

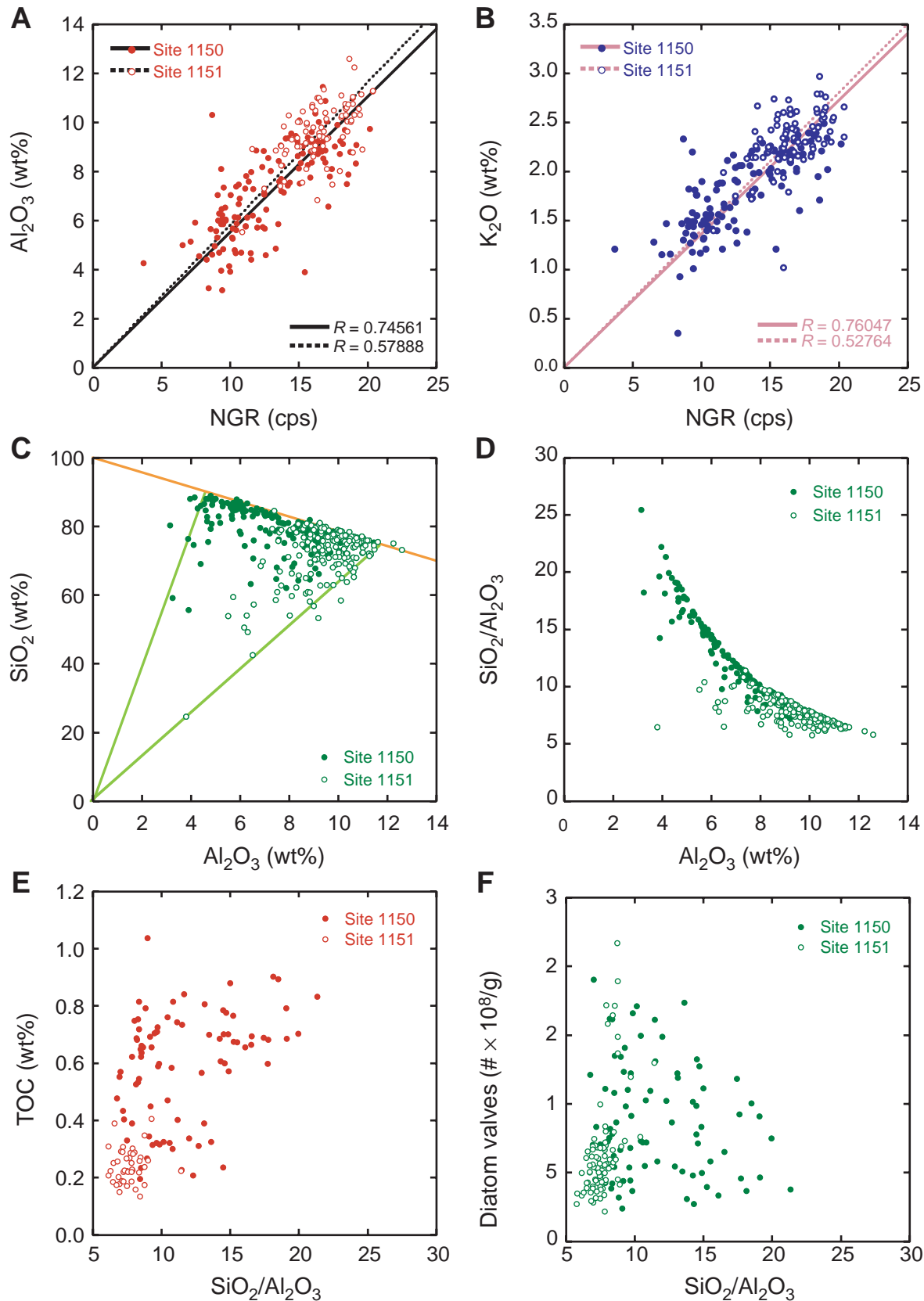


Figure F10. Relationship between natural gamma ray (NGR) intensity and (A) $\text{SiO}_2/\text{Al}_2\text{O}_3$ ratio, (B) porosity, and (C) grain density at Sites 1150 and 1151.

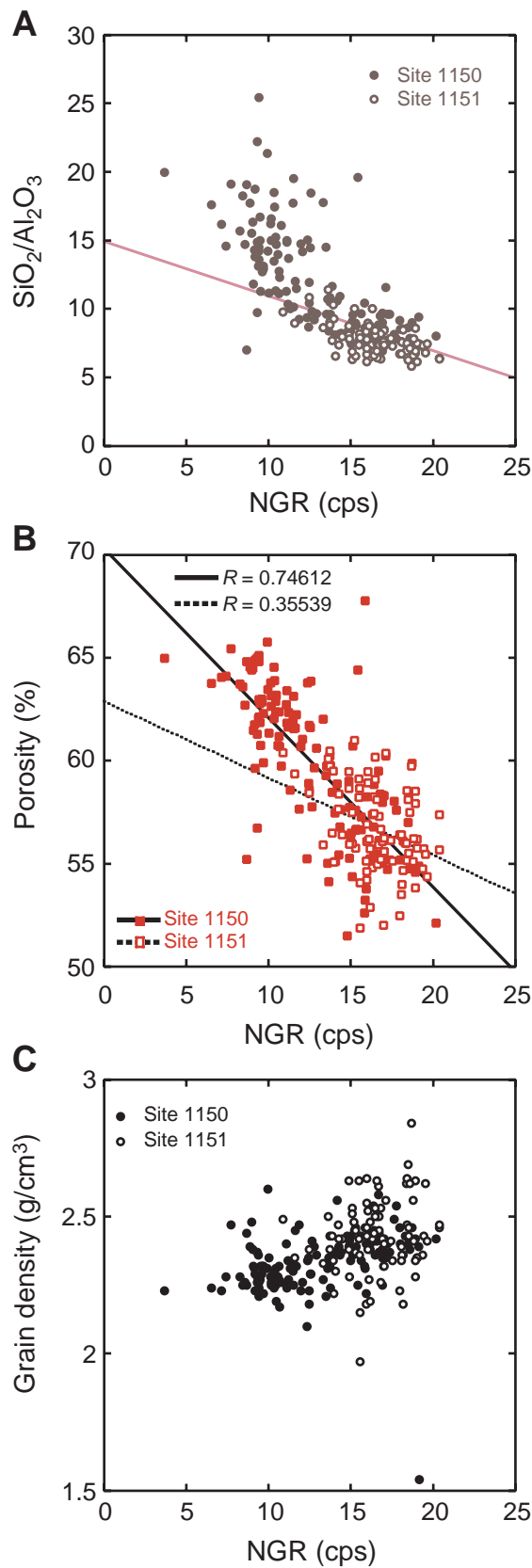


Figure F11. Depth shift and depth adjustment of natural gamma ray (NGR) variations between whole-core MST measurements on sediments from Hole 1150B and wireline logging in Hole 1150D. NGR is plotted with (A, D) logging depth (mbsf) in Hole 1150D, (B, E) tuned depth (meter correlated depth [mcd]) in cores recovered from Hole 1150B to Hole 1150D logging depth, and (C, F) shipboard depth (mbsf) for cores recovered from Hole 1150B.

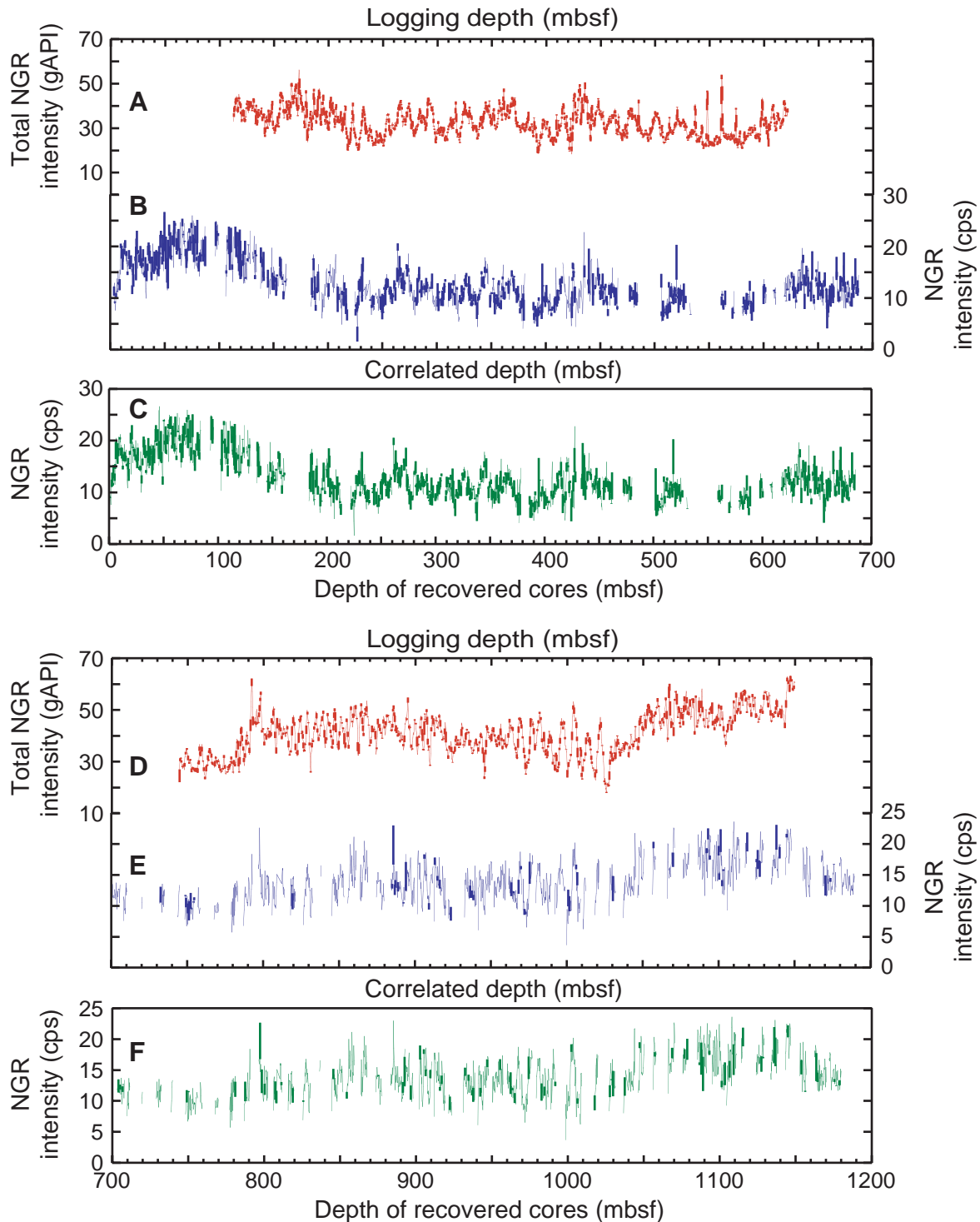


Figure F12. Time serial variation of natural gamma ray (NGR) intensity in Hole 1150D with bandpass filtered components and orbital parameters by Laskar (1993). A. Sedimentation rate (L = low sedimentation rate stage, H = high sedimentation rate stage). B. NGR intensity. C. 20-k.y. bandpass filtering of NGR components. D. Precession index (Laskar, 1993). E. 41-k.y. bandpass filtering of NGR components. F. Obliquity (Laskar, 1993). G. 100-k.y. bandpass filtering of NGR components. H. Eccentricity (Laskar, 1993). I. Power spectral density (PSD) of NGR intensity in each L or H interval (E = periodic components in eccentricity band, O = periodic components in obliquity band, P = periodic components in precession band). ([Figure shown on next page.](#))

Figure F12 (continued). (Caption shown on previous page.)

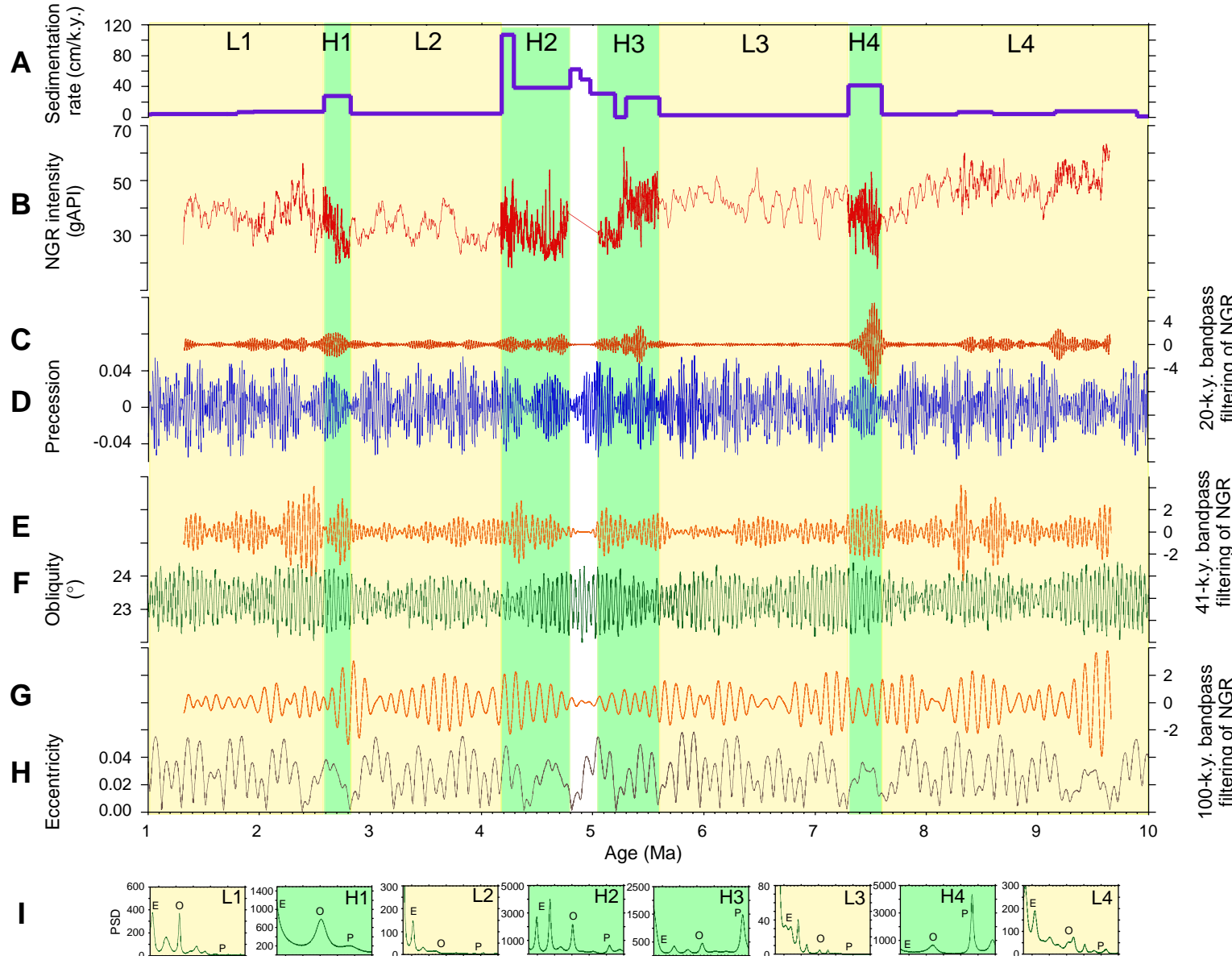


Table T1. Results of major element analysis for bulk samples, Sites 1150 and 1151. (Continued on next four pages.)

Core, section, interval (cm)	Depth (mbsf)	Major element oxide (wt%)									
		Na ₂ O	MgO	Al ₂ O ₃	SiO ₂	S	K ₂ O	CaO	TiO ₂	MnO	Fe ₂ O ₃
186-1150B-											
22R-1, 8-12	902.18	1.99	10.30	72.30	0.50	2.33	6.33	0.64	0.12	5.49	100.00
22R-1, 26-29	902.36	1.80	10.37	72.08	1.66	2.43	4.70	0.72	0.11	6.14	100.00
22R-1, 46-50	902.56	1.53	10.99	74.19	0.44	2.49	3.70	0.70	0.10	5.86	100.00
22R-1, 67-71	902.77	1.67	11.45	75.41	0.29	2.31	2.41	0.68	0.10	5.68	100.00
22R-1, 91-94	903.01	1.69	10.87	75.39	0.73	2.42	1.93	0.68	0.10	6.19	100.00
22R-1, 106-110	903.16	1.50	9.36	76.11	0.75	2.32	2.33	0.63	0.08	6.92	99.99
22R-1, 126-130	903.36	2.06	8.85	79.66	0.33	2.03	1.42		0.11	4.95	99.42
22R-1, 143-147	903.53	1.63	9.22	78.34	0.51	2.15	2.25	0.58	0.08	5.24	100.00
22R-2, 6-10	903.66	1.60	8.55	78.69	0.62	2.06	1.46	0.55	0.08	5.22	98.85
22R-2, 26-30	903.86	1.46	8.24	79.41	0.42	1.98	2.99	0.50	0.09	4.89	99.97
22R-2, 45-49	904.05	2.40	1.33	7.04	78.77	1.46	1.90	1.93	0.48	0.08	4.60
22R-2, 67-71	904.27	1.51	7.34	82.71	0.42	1.81	1.09	0.53	0.08	4.51	100.00
22R-2, 81-84	904.41	1.67	7.96	78.41	0.94	2.12	1.59	0.54	0.09	4.77	98.10
22R-3, 6-10	904.50	1.38	7.03	83.13	0.51	1.82	1.20	0.52	0.07	4.33	100.00
22R-3, 24-28	904.68	2.42	1.21	8.18	76.59	0.54	2.17	2.10	0.50	0.10	4.44
22R-3, 46-50	904.90	1.54	7.15	83.29	0.40	1.82	1.07	0.43	0.09	4.22	100.00
22R-3, 66-70	905.10	1.72	9.02	73.56	1.02	2.30	6.12	0.65	0.10	5.51	100.00
22R-3, 86-90	905.30	1.68	9.69	72.38	0.28	2.39	7.38	0.61	0.09	5.48	99.97
22R-3, 106-110	905.50	1.49	10.03	72.94	0.35	2.37	6.43	0.62	0.10	5.67	100.00
22R-3, 126-130	905.70	2.87	2.00	9.09	70.27	0.90	2.00	4.98	0.61	0.10	5.56
22R-3, 146-150	905.90	2.15	1.63	9.20	66.22	2.94	2.27	6.64	0.57	0.10	5.73
22R-4, 6-10	906.00	3.07	1.96	9.38	73.13	0.25	2.18	4.64	0.48	0.07	4.84
22R-4, 26-30	906.20	2.05	10.08	75.26	0.54	2.26	3.29	0.64	0.08	5.50	99.70
22R-4, 45-49	906.39	1.87	9.34	75.86	0.51	2.23	4.36				94.17
22R-4, 63-66	906.57	7.47	1.28	7.88	62.03	2.33	1.71	5.34		0.08	4.73
22R-4, 86-89	906.80	1.51	9.19	75.03	0.36	2.45	5.47	0.63	0.09	5.24	99.97
22R-5, 6-10	907.00	1.73	9.25	78.87	0.42	2.24	1.33	0.59	5.33		99.77
22R-5, 26-30	907.20	1.93	8.35	79.95	0.46	1.92	2.06	0.60		4.74	100.00
22R-5, 45-49	907.39		7.11	74.21	4.43	2.04	5.89	0.56	0.07	5.36	99.67
22R-5, 66-70	907.60	1.06	7.81	80.67	0.43	1.87	3.11	0.52	0.06	4.47	100.00
22R-5, 84-88	907.78	1.42	7.97	81.04	0.57	1.88	2.03	0.50	0.06	4.54	100.00
22R-5, 104-108	907.98	1.25	7.31	82.47	0.60	1.81	1.60	0.47	0.07	4.44	100.00
22R-5, 123-127	908.17	4.01	1.17	6.20	74.33	0.97	1.67	2.54	0.46	0.07	4.54
22R-5, 143-147	908.37	3.66	0.81	5.18	81.11	0.52	1.43	1.04	0.34	0.05	3.49
22R-6, 6-10	908.48	1.44	6.22	84.53	0.42	1.44	1.47	0.40		4.05	99.97
22R-6, 25-29	908.67	1.37	7.38	83.46	0.31	1.72	1.01	0.49	0.05	4.23	100.00
22R-6, 46-50	908.88	1.19	6.52	82.90	0.44	1.76	2.36	0.46		4.37	100.00
22R-6, 67-71	909.09	2.89	1.50	7.58	76.18	0.85	1.88	1.60	0.46	0.06	4.79
22R-6, 86-90	909.28		7.21	78.02	0.82	1.80	5.27	0.51		4.95	98.58
22R-6, 106-110	909.48	4.49	1.86	8.12	68.19	1.08	1.97	4.58	0.54	0.09	5.33
22R-6, 116-120	909.58	4.70	1.55	7.50	68.12	1.11	2.03	4.47	0.72	0.09	4.84
22R-6, 146-150	909.88	4.43	2.34	8.85	64.58	2.85	2.08	7.40	0.64	0.10	5.84
22R-7, 6-10	909.98	1.65	9.06	75.99	0.52	2.21	4.80	0.60	0.08	5.06	99.98
22R-7, 25-29	910.17	1.48	8.81	76.07	0.42	2.20	4.85	0.64	0.11	5.42	100.00
22R-7, 49-52	910.41	1.76	8.72	74.27	0.57	2.20	5.81	0.57	0.10	5.59	99.60
22R-CC, 5-9	910.59	4.94	1.07	8.21	69.18	0.65	2.28	4.09	0.54	0.08	4.92
28R-4, 6-10	964.24	1.53	7.28	83.44	0.72	1.63	0.64	0.45	0.05	4.24	99.96
28R-4, 27-31	964.45	1.48	7.05	84.06	0.71	1.69	0.60	0.48	0.06	3.86	98.52
28R-4, 46-50	964.64		6.89	84.81	0.86	1.56	0.59	0.43	0.05	4.80	100.00
28R-4, 68-72	964.86		6.13	84.08	2.25	1.56	1.71	0.41	0.05	3.81	100.00
28R-4, 86-90	965.04	3.19	1.48	5.99	78.50	1.93	1.55	1.03	0.29	0.05	3.89
28R-4, 108-111	965.26		5.87	86.37	1.12	1.52	0.84	0.37	0.05	3.85	99.98
28R-4, 126-130	965.44		5.86	87.91	0.45	1.49	0.64	0.37		3.28	100.00
28R-4, 145-149	965.63		4.80	88.82	0.32	1.29	1.34	0.32		3.10	99.99
28R-5, 7-11	965.75	0.83	4.80	88.86	0.59	1.21	0.49	0.34	0.04	2.84	100.00
28R-5, 26-30	965.94	1.37	5.74	86.19	0.77	1.50	0.48	0.44		3.52	100.00
28R-5, 46-50	966.14		5.85	84.85	1.75	1.76	1.48	0.43		3.88	100.00
28R-5, 69-72	966.37	1.40	5.72	84.52	1.34	1.44	0.59	0.41		4.58	100.00
28R-5, 86-90	966.54	1.34	7.43	78.68	2.92	1.99	2.13	0.54	0.05	4.87	99.97
28R-5, 105-109	966.73	1.48	7.75	80.94	0.82	1.85	0.88	0.54	0.06	4.68	99.00
28R-5, 126-130	966.94	1.18	7.80	75.15	3.19	2.24	1.57	0.57		6.35	98.07
28R-5, 146-150	967.14	1.51	9.81	78.61	0.89	2.22	0.81	0.58	0.08	5.48	99.98
28R-6, 7-11	967.25	1.49	8.73	77.96	1.23	2.21	2.13	0.57	0.07	5.62	100.00
28R-6, 26-30	967.44	1.19	8.80	79.13	0.48	2.21	2.38	0.63	0.08	5.11	100.00
28R-6, 46-50	967.64	1.62	9.20	77.08	1.88	2.24	2.04	0.55	0.10	5.29	100.00
28R-6, 66-70	967.84	2.09	10.02	78.41	0.54	2.10	1.03	0.56	0.10	5.16	100.00
28R-6, 89-92	968.07	2.12	9.60	78.50	0.81	1.99	1.08	0.56	0.08	5.07	99.81

Table T1 (continued).

Core, section, interval (cm)	Depth (mbsf)	Major element oxide (wt%)											
		Na ₂ O	MgO	Al ₂ O ₃	SiO ₂	S	K ₂ O	CaO	TiO ₂	MnO	Fe ₂ O ₃		
28R-6, 108–112	968.26		1.31	8.43	81.01	0.68	2.06	0.90	0.56	0.07	4.94	99.97	
28R-6, 128–132	968.46			8.85	81.94	0.80	2.11	0.77	0.50	0.08	4.95	100.00	
28R-CC, 0–4	968.60		1.22	9.29	79.37	1.37	2.38	1.83	0.40	0.10	4.05	100.00	
29R-1, 5–9	969.55		1.11	8.09	78.86	2.00	2.20	2.10	0.56	0.07	5.01	100.01	
29R-1, 28–32	969.78			7.55	82.56	1.21	1.76	0.89	0.54	0.09	5.41	100.00	
29R-1, 46–50	969.96		1.93	7.46	83.13	0.65	1.62	0.72	0.43		3.99	99.94	
29R-1, 71–76	970.21		1.19	6.68	85.26	0.54	1.53	0.64	0.41		3.70	99.96	
29R-1, 86–90	970.36		1.36	6.46	84.81	1.04	1.49	0.85	0.37		3.58	99.96	
29R-1, 106–110	970.56	3.36	1.12	4.84	80.71	1.36	1.34	1.38	0.40	0.07	3.65	94.87	
29R-2, 5–9	970.72		1.33	5.66	83.18	1.06	1.47	0.74	0.39	0.08	3.52	97.45	
29R-2, 23–26	970.90			3.96	87.99	0.70	1.18	1.69	0.28	0.08	3.22	99.10	
29R-2, 46–50	971.13		0.90	6.06	86.23	0.63	1.48	0.55	0.41	0.06	3.67	100.00	
29R-2, 68–72	971.35		1.05	5.31	86.65	0.79	1.44	0.76	0.41		3.60	100.00	
29R-2, 86–90	971.53		0.93	4.62	88.09	0.59	1.30	0.79	0.32		3.37	100.00	
29R-2, 106–110	971.73			4.70	88.10	0.62	1.27	0.64	0.35	0.07	3.23	98.98	
29R-2, 126–131	971.93			5.00	87.98	0.41	1.28	1.59	0.35	0.07	3.32	100.00	
29R-2, 144–146	972.11		1.18	4.88	87.26	0.61	1.36	0.96	0.39		3.36	100.00	
29R-3, 5–9	972.18		1.37	5.26	87.16	0.50	1.32	0.60	0.34	0.06	3.22	99.83	
29R-3, 30–34	972.43		1.42	6.12	85.56	0.42	1.55	0.68	0.41		3.73	99.89	
29R-3, 46–50	972.59		1.41	5.75	85.47	0.69	1.49	0.97	0.42	0.07	3.73	100.00	
29R-3, 66–70	972.79			4.40	69.09	9.20	0.35	11.58	0.50		3.89	99.00	
29R-3, 87–91	973.00		1.35	4.67	81.39	2.34	1.40	3.12	0.34	0.08	3.74	98.44	
29R-3, 113–117	973.26		1.29	5.30	85.88	0.54	1.31	2.15	0.33		3.20	100.00	
29R-3, 126–130	973.39			6.01	87.12	0.38	1.35	0.97	0.43	0.07	3.51	99.85	
29R-3, 146–150	973.59		1.37	6.70	83.80	0.47	1.62	1.61	0.45		3.99	100.00	
29R-4, 6–10	973.69		0.91	5.68	82.20	1.14	1.40	3.70	0.43	0.08	4.46	100.00	
29R-4, 26–30	973.89		0.98	7.70	81.07	0.69	1.73	2.58	0.46	0.12	4.67	100.00	
29R-4, 50–54	974.13		1.34	7.58	81.26	0.61	2.17	1.92	0.55		4.57	100.00	
29R-4, 65–70	974.28		1.51	6.56	75.90	0.65	1.60	8.99	0.47	0.09	4.23	100.00	
29R-4, 86–90	974.49	3.44	1.47	7.48	64.64	4.44	1.95	6.41	0.62	0.09	5.34	92.45	
29R-4, 106–110	974.69		3.00	1.99	8.62	74.05	1.40	1.99	1.86	0.55	0.10	4.68	95.23
29R-4, 126–130	974.89		1.70	9.54	78.56	0.91	2.29	1.04	0.54	0.09	5.29	99.97	
29R-4, 144–150	975.07		1.19	9.13	78.55	0.96	2.17	1.83	0.63	0.10	5.42	100.00	
29R-5, 6–10	975.19		1.88	9.45	78.35	0.55	2.19	1.50	0.57	0.11	5.26	99.86	
29R-5, 24–28	975.37		1.49	9.04	79.44	0.63	2.22	1.18	0.65	0.10	5.02	99.77	
29R-5, 46–50	975.59	3.94	1.43	8.91	71.78	1.27	2.09	2.62	0.57	0.09	4.94	93.71	
29R-5, 66–70	975.79		1.91	9.34	79.51	0.68	2.17	0.90	0.59		4.69	99.80	
29R-5, 86–90	975.99		1.57	8.53	80.95	0.61	2.17	1.13	0.54	0.10	4.41	100.00	
29R-5, 110–114	976.23		1.75	9.13	78.09	1.51	2.36	1.64	0.49	0.11	4.07	99.14	
29R-5, 126–130	976.39		1.51	8.37	81.28	0.52	2.00	1.23	0.54		4.56	100.00	
29R-6, 6–10	976.58	1.45	1.77	7.80	70.73	3.84	2.11	3.44	0.54	0.13	5.28	95.64	
29R-6, 29–34	976.81		1.46	6.83	79.64	2.40	1.78	0.84	0.54		4.94	98.44	
29R-6, 46–50	976.98		1.36	6.98	83.72	0.82	1.70	0.80	0.46		4.16	100.00	
29R-6, 65–70	977.17	5.06	1.63	6.53	70.69	3.43	1.63	1.12	0.40	0.14	4.74	90.31	
29R-6, 86–90	977.38		1.13	6.60	83.99	0.11	1.64	0.96	0.40	0.08	4.00	98.90	
29R-6, 106–110	977.58		1.61	7.58	79.15	2.60	0.85	1.94	0.55	0.10	4.61	99.00	
29R-6, 126–129	977.78		1.21	8.73	80.78	1.11	1.94	1.30	0.48	0.07	4.38	100.00	
29R-CC, 6–10	977.87		1.11	7.29	83.90	0.68	1.81	0.74	0.45		4.02	100.00	
186-1151B-													
32R-1, 9–12	998.39		1.22	4.27	85.23	0.86	1.21	1.13	0.29		2.84	97.07	
32R-1, 25–29	998.55	4.35	1.65	3.16	80.33	1.32	1.01	0.78	0.23	0.09	2.43	91.00	
32R-1, 44–47	998.74			4.54	86.64	0.96	1.16	0.52	0.28	0.10	4.02	98.22	
32R-1, 67–70	998.97		2.55	1.32	5.13	82.90	0.68	1.15	0.96	0.34	0.06	3.19	95.72
32R-1, 87–90	999.17		1.04	4.15	88.48	0.45	1.17	1.43	0.36		2.93	100.00	
32R-1, 107–110	999.37		1.41	4.59	84.73	0.58	1.27	3.47	0.36	0.09	3.50	99.99	
32R-1, 123–127	999.53	3.51	1.21	4.11	74.62	1.04	1.17	8.02	0.35	0.09	2.93	93.54	
32R-2, 7–10	999.71		10.40	1.24	3.25	59.20	3.85	0.93	6.23	0.25	2.42	77.37	
32R-2, 29–32	999.93		1.24	6.00	85.97	0.58	1.49	0.71	0.43		3.58	100.00	
32R-2, 46–50	1000.1		1.40	4.40	85.93	0.44	1.21	3.06	0.33		3.22	100.00	
32R-2, 66–70	1000.3		1.87	6.15	82.82	0.76	1.56	1.39	0.48		3.65	98.67	
32R-2, 86–90	1000.5			3.91	55.69	12.93	1.46	14.29	0.43	0.11	4.09	92.91	
32R-2, 106–110	1000.7	4.62	1.49	4.69	75.48	1.61	1.41	1.75	0.34	0.10	3.11	89.97	
32R-2, 126–130	1000.9			6.29	86.78	0.47	1.47	0.67	0.48		3.84	100.00	
32R-3, 6–10	1001.15			5.85	87.05	0.72	1.58	0.78	0.40		3.59	99.97	
32R-3, 25–29	1001.34		1.16	6.01	85.14	0.74	1.63	0.85	0.42	0.09	3.97	100.00	
32R-3, 47–50	1001.56	3.90	1.62	6.44	63.19	8.51	1.89	5.61	0.49	0.15	5.85	93.74	
32R-3, 66–69	1001.75		1.43	8.27	79.95	1.34	2.12	1.39	0.63	0.07	4.80	100.00	
32R-3, 86–90	1001.95		1.35	9.20	77.91	1.37	2.18	1.60	0.55		5.83	100.00	
32R-3, 107–110	1002.16		1.63	8.33	78.34	1.82	2.34	1.57	0.52		5.46	100.00	

Table T1 (continued).

Core, section, interval (cm)	Depth (mbsf)	Major element oxide (wt%)										
		Na ₂ O	MgO	Al ₂ O ₃	SiO ₂	S	K ₂ O	CaO	TiO ₂	MnO	Fe ₂ O ₃	
32R-3, 126–130	1002.35		1.56	8.72	79.85	0.82	2.31	0.90	0.59	0.08	5.15	100.00
32R-3, 141–145	1002.5	3.81	1.45	9.15	72.21	1.64	2.83	0.93	0.50	0.11	4.46	93.28
32R-4, 9–13	1002.64		1.63	9.23	76.57	2.08	2.15	1.76	0.59	0.10	5.89	100.00
32R-4, 27–30	1002.82	3.19	1.93	9.07	67.73	4.14	2.02	3.18	0.64	0.10	6.30	95.11
32R-4, 47–50	1003.02		1.68	9.25	78.79	0.90	2.18	0.99	0.51	0.09	5.63	100.00
32R-4, 68–71	1003.23	3.51	1.65	9.57	71.60	2.08	2.22	1.78	0.67	0.10	5.14	94.80
32R-4, 88–91	1003.43		2.01	8.10	77.89	2.06	2.18	1.45	0.57		5.71	99.96
32R-4, 106–110	1003.61		1.80	9.73	77.94	1.15	2.28	1.03	0.59	0.06	5.40	99.98
32R-4, 126–130	1003.81		2.21	9.89	77.52	0.68	2.39	1.01	0.65	0.08	5.57	99.99
32R-4, 146–150	1004.01		2.03	11.03	76.55	0.47	2.51	1.01	0.67	0.10	5.65	100.00
32R-5, 7–10	1004.12		1.51	9.21	76.99	1.78	2.33	1.22	0.53	0.06	5.73	99.38
32R-5, 27–30	1004.32	4.26	1.65	8.37	64.20	4.90	2.21	3.82	0.51	0.14	5.38	91.18
32R-5, 47–50	1004.52		1.03	8.82	78.11	1.55	2.17	1.18	0.58		5.32	98.77
32R-5, 67–70	1004.72		1.55	8.84	76.50	1.77	1.91	1.82	0.63	0.10	6.89	100.00
32R-5, 87–90	1004.92		1.43	8.01	77.47	2.58	2.06	2.85	0.54		5.06	100.00
32R-5, 108–112	1005.13	4.40	0.93	3.89	76.36	1.35	1.21	2.48	0.33		2.86	89.40
32R-5, 125–130	1005.3		1.04	4.86	86.31	1.01	1.38	0.85	0.44		3.59	99.48
32R-5, 139–143	1005.44		1.05	5.89	85.69	0.84	1.42	0.99	0.40		3.73	100.00
32R-6, 6–9	1005.61			5.91	86.30	0.82	1.47	0.89	0.41		4.05	99.87
32R-6, 26–29	1005.81		1.58	5.68	85.16	0.81	1.50	0.66	0.37	0.07	4.16	100.00
32R-6, 47–50	1006.02		4.67	82.71	2.73	1.54	3.96	0.56		3.66	99.83	
32R-6, 86–89	1006.41		1.45	5.62	85.63	0.72	1.45	0.65	0.43	0.08	3.96	99.99
32R-6, 104–106	1006.59		0.94	4.96	87.97	0.51	1.37	0.63	0.39		3.23	100.00
32R-6, 124–127	1006.79		1.27	5.57	86.45	0.38	1.50	0.80	0.39	0.05	3.58	100.00
32R-6, 146–150	1007.01		1.16	5.47	86.81	0.61	1.54	0.61	0.37	0.07	3.37	100.01
32R-7, 6–9	1007.11	2.58	1.38	6.03	77.84	2.17	1.76	1.84	0.39	0.07	3.56	95.02
32R-7, 27–30	1007.32		1.23	5.77	86.52	0.37	1.40	0.80	0.45		3.46	100.00
32R-7, 46–49	1007.51	1.99	1.30	4.80	79.26	2.18	1.33	1.37	0.30	0.09	4.12	94.75
32R-CC, 7–10	1007.67		1.12	5.72	86.93	0.47	1.32	0.61	0.38		3.43	100.00
186-1151A-												
91R-1, 19–23	930.59		1.81	10.61	73.84	0.78	2.47	3.84	0.63	0.11	5.91	100.00
91R-1, 29–32	930.69		1.97	10.03	72.39	0.95	2.46	5.93	0.67	0.09	5.52	100.00
91R-1, 39–42	930.79		1.38	10.05	71.16	1.22	2.48	7.64	0.68	0.13	5.25	100.00
91R-1, 46–49	930.86		1.99	11.26	72.10	0.39	2.35	5.36	0.59	0.10	5.85	100.00
91R-1, 55–59	930.95		2.46	10.37	71.09	1.69	2.63	4.82	0.73	0.11	6.09	100.00
91R-1, 64–67	931.04		1.71	10.99	72.34	1.66	2.73	3.93	0.78	0.11	5.76	100.01
91R-1, 77–81	931.17		1.24	9.53	63.02	4.79	2.42	8.43	0.91	0.11	6.21	96.65
91R-1, 88–91	931.28		2.26	11.34	71.85	1.35	2.42	2.65	0.67	0.11	5.97	98.61
91R-1, 99–102	931.39		1.55	8.87	76.28	0.91	2.11	4.68	0.50	0.10	5.00	100.00
91R-1, 108–111	931.48		1.63	9.79	76.00	0.71	2.14	2.91	0.67	0.10	6.05	100.00
91R-1, 118–121	931.58		1.67	9.34	77.57	0.35	2.26	3.14	0.60		5.07	100.00
91R-1, 127–131	931.67		1.52	9.37	75.78	0.78	2.20	4.33	0.59	0.10	5.33	100.00
91R-1, 137–140	931.77		2.15	9.33	73.15	0.94	2.10	5.55	0.64	0.10	5.15	99.10
91R-1, 145–149	931.85		1.60	8.74	73.35	0.91	2.17	7.91	0.60	0.09	4.62	99.98
91R-2, 8–12	931.98		1.41	8.86	69.12	1.81	2.24	8.69	0.67	0.16	5.46	98.42
91R-2, 20–23	932.1		1.41	8.28	62.18	4.97	2.24	10.14	0.62	0.14	6.55	96.53
91R-2, 31–34	932.21		1.29	9.04	73.14	0.52	2.20	8.30	0.55	0.10	4.86	100.00
91R-2, 41–43	932.31		1.71	8.40	65.78	2.34	2.29	8.61	0.47	0.14	8.57	98.32
91R-2, 50–53	932.4		1.65	10.49	67.78	1.61	2.47	8.30	0.66	0.22	6.14	99.32
91R-2, 58–61	932.48			6.52	42.48	12.21	1.93	18.54	1.02	0.15	7.30	90.15
91R-2, 70–73	932.6			9.01	56.80	5.78	2.42	10.66	0.84	0.18	7.92	93.63
91R-2, 78–81	932.68		1.73	10.67	67.95	1.11	2.43	8.96	0.67	0.14	6.35	100.00
91R-2, 87–90	932.77		1.78	10.54	69.24	1.27	2.60	7.86	0.70	0.12	5.86	99.97
91R-2, 97–100	932.87	8.27	1.67	9.19	53.40	2.50	2.00	8.42	0.52	0.09	4.86	82.65
91R-2, 108–111	932.98		1.73	9.80	63.01	4.24	2.59	11.47	0.73	0.11	6.32	100.00
91R-2, 117–120	933.07		1.53	10.29	69.25	0.50	2.56	8.78	0.65	0.13	6.31	100.00
91R-2, 127–130	933.17		1.89	10.61	70.99	1.02	1.02	5.07	0.72	0.10	6.87	98.29
91R-2, 145–148	933.35		1.24	10.67	74.01	0.31	2.47	5.70	0.56	0.13	4.91	100.00
91R-3, 8–11	933.48		1.74	9.31	74.36	0.53	2.14	6.00	0.63	0.08	5.20	99.98
91R-3, 18–21	933.58		1.31	7.62	66.93	2.24	1.86	10.18	0.50	0.12	5.54	96.31
91R-3, 26–29	933.66		1.57	9.62	73.26	0.83	2.33	6.61	0.66	0.08	5.01	99.97
91R-3, 38–41	933.78		1.68	11.00	73.67	0.43	2.54	4.65	0.68	0.11	5.26	100.02
91R-3, 48–51	933.88		1.22	10.30	74.13	0.16	2.30	6.27	0.66	0.07	4.88	100.00
91R-3, 59–62	933.99		1.64	10.25	70.83	2.81	2.39	5.55	0.63	0.09	5.80	100.00
91R-3, 66–70	934.06		1.94	10.28	75.66	0.89	2.33	2.69	0.60	0.07	5.53	100.00
91R-3, 78–81	934.18	2.97	1.17	9.15	71.50	0.97	1.97	4.85	0.57	0.10	5.00	95.28
91R-3, 88–91	934.28		1.00	8.25	74.61	0.88	1.79	6.80	0.42	0.13	6.10	99.96
91R-3, 98–101	934.38		1.57	8.41	71.55	2.31	2.30	7.25	0.69	0.18	5.68	99.94
91R-3, 107–110	934.47			6.84	68.50	4.48	1.79	9.50	0.60	0.14	6.10	97.95

Table T1 (continued).

Core, section, interval (cm)	Depth (mbsf)	Major element oxide (wt%)										
		Na ₂ O	MgO	Al ₂ O ₃	SiO ₂	S	K ₂ O	CaO	TiO ₂	MnO	Fe ₂ O ₃	
91R-3, 117–120	934.57	5.01	1.36	7.67	62.73	2.33	2.06	9.29	0.56	0.09	4.54	90.62
91R-3, 139–142	934.79		1.43	10.35	63.85	3.34	2.33	11.82	0.65		6.12	99.89
91R-3, 146–149	934.86	3.61	1.84	10.16	64.93	0.76	2.38	7.88	0.66	0.08	4.96	93.66
91R-4, 7–10	934.97		1.80	10.01	66.10	1.61	2.53	8.71	0.64	0.11	5.66	97.16
91R-4, 17–20	935.07		1.53	9.89	71.13	1.01	2.53	6.99	0.70	0.10	6.13	100.00
91R-4, 27–30	935.17		1.92	11.28	71.46	0.27	2.66	5.95	0.66	0.07	5.73	100.00
91R-4, 37–40	935.27		1.83	10.35	72.09	1.60	2.45	5.03	0.69		5.88	99.91
91R-4, 48–51	935.38		1.18	9.37	72.14	1.01	2.28	8.12	0.58	0.08	5.24	100.00
91R-4, 59–62	935.49		1.69	10.04	77.39	0.69	2.14	1.82	0.64		5.59	100.00
91R-4, 67–70	935.57		1.15	9.04	79.84	0.65	2.14	1.24	0.60	0.08	5.26	100.00
91R-4, 79–82	935.69		1.05	9.85	77.12	0.66	2.27	2.92	0.63	0.11	5.36	99.96
91R-4, 88–92	935.78	3.39	1.32	7.55	75.73	1.11	1.89	2.39	0.47	0.06	4.43	94.94
91R-4, 97–100	935.87		1.44	9.22	80.61	0.44	2.05	1.20	0.53	0.08	4.44	100.00
91R-4, 107–110	935.97		1.49	7.59	78.26	1.28	2.14	3.81	0.42		4.52	99.51
91R-4, 117–120	936.07		0.78	8.05	79.03	1.53	2.12	2.46	0.50	0.08	5.44	100.00
91R-4, 127–130	936.17		1.23	8.60	76.85	2.34	2.28	2.46	0.54	0.08	5.58	99.96
91R-4, 137–140	936.27		1.20	8.58	79.28	0.78	2.21	2.11	0.49		5.35	100.00
91R-4, 147–150	936.37		1.90	10.49	76.64	0.41	2.34	2.58	0.60		5.05	100.00
91R-5, 7–10	936.47	4.33	1.68	9.41	69.41	0.79	2.34	4.30	0.57	0.07	4.70	93.28
91R-5, 19–22	936.59		1.01	10.60	76.12	0.30	2.62	4.23	0.60	0.07	4.41	99.96
91R-5, 30–34	936.67	2.69	1.46	9.84	75.80	0.83	2.41	1.42	0.48	0.08	4.98	97.31
91R-5, 37–40	936.77		2.20	10.76	75.31	1.05	2.49	1.71	0.67	0.08	5.71	99.97
91R-5, 49–53	936.89		1.61	10.71	76.45	0.59	2.60	1.60	0.72	0.07	5.61	99.95
91R-5, 59–62	936.99		1.81	10.06	77.01	1.06	2.27	1.82	0.65	0.07	5.25	100.01
91R-5, 69–72	937.09		1.75	10.96	75.85	0.76	2.64	1.50	0.63		5.90	100.00
91R-5, 79–82	937.19		2.01	11.48	73.27	1.20	2.58	1.66	0.67	0.09	7.04	100.00
91R-5, 89–92	937.29		1.88	11.00	72.43	2.44	2.58	2.72	0.71	0.09	6.14	99.98
91R-5, 98–101	937.38	1.71	1.69	9.92	68.98	2.40	2.37	3.71	0.62	0.07	5.47	95.23
91R-5, 109–112	937.49		1.64	9.16	70.52	4.25	2.53	4.93	0.71	0.10	6.12	99.97
91R-5, 119–122	937.59		1.58	10.64	76.59	0.71	2.54	1.40	0.64	0.10	5.67	99.87
91R-5, 129–133	937.69		1.61	10.45	68.38	3.14	2.74	4.43	0.76		7.31	98.81
91R-5, 139–142	937.79		2.13	10.71	75.24	1.23	2.52	1.93	0.60	0.09	5.53	99.99
91R-5, 147–150	937.87	6.29	1.87	9.27	62.86	2.14	2.21	3.21	0.59	0.09	5.01	87.25
91R-6, 32–35	938.22	5.05	1.20	10.02	69.03	0.77	2.22	2.62	0.58	0.09	4.76	91.28
91R-6, 42–45	938.32	0.73	1.29	9.17	76.74	1.82	2.44	1.88	0.65	0.09	5.15	99.22
91R-6, 50–54	938.4	6.77	1.69	8.11	66.31	2.33	2.00	2.34	0.48	0.10	4.29	87.65
91R-6, 60–63	938.5		1.74	8.29	78.33	1.40	2.02	1.53	0.52	0.09	6.06	99.99
91R-6, 72–75	938.62		1.25	8.92	80.01	0.93	1.99	0.84	0.53		5.51	99.98
91R-6, 84–86	938.74		1.81	8.63	80.33	0.35	1.97	1.51	0.51	0.07	4.71	99.89
91R-6, 94–97	938.84	10.36	1.07	5.52	53.85	3.94	1.40	7.40	0.47	0.11	4.44	78.21
91R-6, 101–104	938.91		1.28	7.68	79.06	1.20	1.20	3.85	0.47	0.09	4.49	99.33
91R-6, 110–113	939		1.14	7.31	79.32	0.44	1.75	5.17	0.48			95.61
91R-6, 119–122	939.09		1.26	6.92	69.80	3.40	2.04	7.74	0.92	0.11	4.78	96.97
91R-6, 128–131	939.18			8.86	76.63	1.20	2.13	5.03	0.60	0.11	5.44	100.00
91R-6, 137–140	939.27	12.48		6.27	54.09	3.17	1.55	7.85	0.45	0.10	3.78	77.26
91R-CC, 6–9	939.39		1.12	9.20	73.94	0.92	2.01	5.61	0.64	0.11	5.12	98.68
91R-CC, 18–21	939.51		1.47	8.53	74.81	0.73	2.04	6.84	0.59	0.10	4.90	100.00
105R-1, 6–9	1065.36		1.36	8.85	58.13	9.75	2.67	9.19			7.46	97.43
105R-1, 18–21	1065.48		1.31	9.85	77.67	0.83	2.44	1.71	0.61		5.55	99.97
105R-1, 28–31	1065.58		1.53	9.31	77.82	0.93	2.34	1.48	0.55		6.00	99.96
105R-1, 38–41	1065.68		1.71	9.57	74.63	1.27	2.55	1.96	0.60		5.74	98.03
105R-1, 49–51	1065.79		1.54	8.72	80.93	0.22	2.26	1.00	0.56		4.74	99.97
105R-1, 56–60	1065.86		1.54	9.50	79.85	0.44	2.21	1.09	0.57		4.76	99.97
105R-1, 69–72	1065.99		1.34	9.40	79.80	0.27	2.42	1.34	0.55		5.06	100.18
105R-1, 79–82	1066.09	2.24	0.96	7.97	71.09	2.49	2.30	2.52	0.33		4.75	92.41
105R-1, 88–91	1066.18		1.54	9.92	78.18	0.34	2.58	1.25	0.58		5.57	99.97
105R-1, 97–100	1066.27		1.96	10.59	77.17	0.54	2.46	1.08	0.54		5.67	100.00
105R-1, 110–112	1066.4	9.74		7.46	58.66	3.45	2.12	4.74	0.41		4.53	81.37
105R-1, 119–122	1066.49	6.43	1.48	10.75	70.77	1.76	2.30	2.59	0.52			90.17
105R-1, 130–133	1066.6		1.68	12.24	75.06	0.21	2.76	1.31	0.64			100.00
105R-1, 137–140	1066.67		1.88	11.26	75.86	0.36	2.64	1.17	0.54		6.29	100.00
105R-1, 146–149	1066.76		1.45	10.83	76.22	0.94	2.35	1.18	0.52		6.51	100.00
105R-2, 8–11	1066.88		1.72	9.62	70.83	3.39	2.47	2.42			6.57	97.01
105R-2, 17–20	1066.97	0.83	1.59	9.94	76.06	0.90	2.54	1.69	0.60		5.07	98.40
105R-2, 27–30	1067.07		1.96	10.20	77.53	0.82	2.26	1.43	0.57	0.06	5.17	100.00
105R-2, 37–40	1067.17		1.26	10.67	76.93	0.61	2.40	1.32	0.59	0.06	6.15	100.00
105R-2, 46–49	1067.26		1.57	10.39	77.34	0.30	2.61	1.67	0.62	0.08	5.43	100.00
105R-2, 57–60	1067.37		1.20	10.46	78.39	0.18	2.32	1.17	0.59	0.06	5.61	99.98
105R-2, 67–70	1067.47		1.61	10.76	76.76	0.29	2.61	1.34	0.61	0.06	5.98	99.95

Table T1 (continued).

Core, section, interval (cm)	Depth (mbsf)	Major element oxide (wt%)										
		Na ₂ O	MgO	Al ₂ O ₃	SiO ₂	S	K ₂ O	CaO	TiO ₂	MnO	Fe ₂ O ₃	
105R-2, 77–80	1067.57		1.78	10.13	77.68	0.41	2.26	1.62	0.55	0.06	5.52	100.00
105R-2, 87–89	1067.67		1.70	12.59	73.19	0.57	2.79	1.79	0.67		6.71	100.00
105R-2, 97–100	1067.77		1.73	11.62	75.46	0.29	2.56	1.37	0.64		6.34	100.00
105R-2, 107–110	1067.87		1.23	11.03	76.51	0.55	2.55	1.47	0.63	0.10	5.93	99.99
105R-2, 117–120	1067.97		1.40	10.35	74.95	0.93	2.54	1.88	0.62	0.07	7.27	100.00
105R-2, 130–133	1068.1		1.90	10.54	77.14	0.34	2.41	1.58	0.60	0.06	5.43	100.00
105R-2, 137–140	1068.17		1.38	10.16	78.51	0.38	2.31	1.35	0.66	0.07	4.98	99.80
105R-2, 147–149	1068.27		2.04	9.98	78.36	0.57	2.13	1.43	0.51	0.05	4.89	99.96
105R-3, 7–10	1068.37		2.05	10.01	78.13	0.22	2.23	1.25	0.55		5.56	100.00
105R-3, 18–21	1068.48		1.59	10.33	77.36	0.49	2.44	1.74	0.60	0.07	5.38	100.00
105R-3, 26–29	1068.56	3.39	1.83	10.64	65.29	2.65	1.94	3.30	0.65	0.20	6.96	93.47
105R-3, 38–41	1068.68		1.82	9.70	77.03	0.86	2.39	1.60	0.59	0.05	5.95	100.00
105R-3, 50–52	1068.8		1.61	9.98	78.94	0.46	2.13	0.99	0.61		5.26	99.97
105R-3, 58–61	1068.88	11.56	0.99	6.17	50.54	4.34	1.93	4.98	0.43		5.61	75.00
105R-3, 68–70	1068.98	0.65	1.54	9.32	78.63	0.96	2.16	1.86	0.53		4.34	99.34
105R-3, 79–82	1069.09	3.53	1.55	9.35	70.06	1.31	2.40	2.55	0.55	0.06	5.40	93.22
105R-3, 87–90	1069.17		1.87	10.48	76.57	0.95	2.30	1.75	0.55	0.05	5.05	99.57
105R-3, 97–100	1069.27	4.73	1.80	8.86	69.46	1.17	2.32	1.92	0.54		5.56	91.63
105R-3, 105–107	1069.35		1.06	10.26	77.55	0.32	2.23	1.56	0.63	0.04	5.81	99.48
105R-3, 115–118	1069.45		1.52	10.97	77.11	0.39	2.31	1.48	0.61		5.58	99.97
105R-3, 126–129	1069.56		2.02	10.86	75.30	0.28	2.44	1.72	0.64	0.07	6.67	100.00
105R-3, 138–141	1069.68	3.59	1.54	9.78	68.01	2.15	2.34	3.24	0.54	0.07	5.85	93.52
105R-3, 147–150	1069.77	29.44		3.80	24.65	4.27	1.09	6.06	0.28		4.83	44.99
105R-4, 7–10	1069.88	9.78	1.60	8.02	54.05	3.23	2.15	4.15	0.51	0.07	6.66	80.45
105R-4, 16–18	1069.97		1.63	10.65	75.94	0.77	2.51	1.76	0.62	0.06	6.06	100.00
105R-4, 26–29	1070.07		1.59	10.76	74.73	0.86	2.64	1.91	0.55	0.55	6.85	100.43
105R-4, 36–39	1070.17		1.96	10.78	75.98	0.65	2.49	1.74	0.55	0.06	5.71	99.91
105R-4, 47–50	1070.28		2.04	11.10	74.47	0.70	2.46	1.98	0.55	0.07	6.59	99.97
105R-4, 56–59	1070.37	5.75	1.44	8.67	60.51	4.36	2.17	5.33	0.51		5.30	88.29
105R-4, 64–67	1070.45		1.63	11.13	75.97		2.52	1.07	0.67	0.07	6.54	99.60
105R-4, 78–81	1070.59		1.89	10.24	73.40	1.29	2.52	1.76	0.65	0.07	7.33	99.15
105R-4, 87–90	1070.68		1.75	10.15	77.23	0.70	2.32	1.52	0.74	0.06	5.50	99.97
105R-4, 96–99	1070.77	5.36	1.71	9.05	70.38	0.78	2.15	1.84	0.52	0.04	5.20	91.69
105R-4, 107–110	1070.88	2.98	1.61	8.89	66.12	3.53	2.55	4.00	0.50	0.06	6.68	93.93
105R-4, 117–120	1070.98	3.52	1.08	8.76	60.86	5.77	2.55	6.32	0.50	0.07	8.01	93.94
105R-4, 130–133	1071.11	3.77	1.15	10.61	66.69	1.93	2.45	3.08	0.52	0.10	6.55	93.07
105R-4, 138–141	1071.19		1.77	11.45	74.43	0.46	3.01	1.98	0.69	0.07	6.21	100.07
105R-4, 147–150	1071.28	nd	1.44	11.19	75.97	0.91	2.77	2.01	0.55	0.07	4.79	99.70
105R-5, 7–10	1071.38		1.46	9.62	78.78	0.29	2.49	1.26	0.53	0.06	5.51	100.00
105R-5, 17–20	1071.48		1.88	10.05	78.65	0.12	2.28	1.25	0.58	0.05	5.15	100.00
105R-5, 28–30	1071.59		1.63	10.31	77.23	0.39	2.65	1.54	0.48	0.04	5.36	99.63
105R-5, 35–39	1071.66	13.98		6.31	49.29	3.46	1.89	4.89	0.35		4.76	70.93
105R-5, 49–52	1071.8		1.08	8.77	75.49	2.08	2.28	2.68	0.68	0.06	4.80	97.91
105R-5, 57–60	1071.88		1.54	8.90	80.36	0.26	2.16	1.10	0.54	0.08	4.96	99.90
105R-5, 69–73	1072		1.37	10.08	78.72	0.20	2.58	1.26	0.52	0.09	5.17	100.00
105R-5, 77–80	1072.08		1.33	9.90	74.05	1.57	2.52	2.24	0.70	0.12	6.48	98.89
105R-5, 87–90	1072.18		1.42	10.30	77.35	0.37	2.79	1.27	0.66	0.09	5.70	99.95
105R-5, 97–100	1072.28		2.01	10.45	75.81	0.25	2.61	1.37	0.62	0.14	6.72	99.97
105R-5, 107–110	1072.38			10.73	76.68	0.55	2.97	2.45	0.94	0.11	5.56	99.97
105R-5, 118–122	1072.49	8.71		7.51	60.84	2.85	2.10	3.99	0.42	0.07	4.41	82.19
105R-5, 127–130	1072.58	5.94	1.01	8.10	59.73	4.76	2.30	5.69	0.46	0.13	5.70	87.87
105R-5, 137–140	1072.68	4.98	1.22	8.84	60.82	4.58	2.16	4.58	0.51	0.12	6.19	89.01
105R-5, 147–150	1072.78		1.75	10.11	58.40	8.04	2.58	10.02	0.68	0.17	7.11	98.85
105R-6, 8–12	1072.89		1.21	9.06	79.50	0.65	2.41	1.32	0.62		5.18	99.94
105R-6, 17–20	1072.98		1.62	9.36	72.96	1.82	2.35	2.46	0.50	0.13	6.03	97.22
105R-6, 27–30	1073.08		1.74	9.01	79.03	1.26	2.25	1.72	0.59		4.40	100.00
105R-6, 37–40	1073.18	4.19	1.20	8.68	65.02	4.48	2.00	4.51	0.55	0.16	5.95	92.54
105R-6, 60–63	1073.41	10.36		5.72	59.51	3.24	1.51	4.19	0.27		3.59	78.04
105R-6, 67–70	1073.48		1.27	7.40	84.57	0.27	1.72	0.93	0.35		3.47	99.98
105R-6, 78–81	1073.59		1.56	9.31	79.60	0.41	2.26	1.33	0.45	0.09	4.99	100.00
105R-6, 87–90	1073.68		1.03	8.87	77.70	0.57	2.38	1.01	0.40	0.13	6.87	98.97
105R-6, 99–102	1073.8		1.03	8.37	80.66	1.01	2.17	0.39	0.60	0.09	4.68	99.00
105R-6, 107–110	1073.88		1.56	9.57	77.00	1.05	2.58	1.91	0.49	0.11	5.73	100.00
105R-6, 117–120	1073.98			9.26	81.11	0.30	2.19	1.10	0.50	0.13	5.37	99.96
105R-6, 127–130	1074.08		1.72	9.44	79.39	0.42	2.12	1.53	0.50		4.89	100.00
105R-6, 137–140	1074.18	4.54	1.16	6.56	57.23	8.04	1.96	7.48	0.40	0.14	5.37	88.33
105R-CC, 6–9	1074.31		1.70	9.80	77.75	0.87	2.33	1.35	0.50		4.90	99.20
105R-CC, 15–18	1074.4		1.66	8.17	79.48	1.17	1.92	1.97	0.58		5.06	100.01

Table T2. Results of physical properties for bulk samples, Sites 1150 and 1151.
(Continued on next five pages.)

Core, section, interval (cm)	Depth (mbsf)	Salinity (%)	Water content		Density (g/cm ³)			Porosity (%)	Void ratio
			(% of total mass)	(% of total solids)	Bulk	Dry	Grain		
186-1150B-									
22R-1, 8–12	902.18	1.8	34.04	51.61	1.66	1.10	2.44	55.20	1.23
22R-1, 26–29	902.36	1.8	34.46	52.57	1.64	1.08	2.40	55.22	1.23
22R-1, 46–50	902.56	1.8	33.74	50.92	1.66	1.10	2.42	54.58	1.20
22R-1, 67–71	902.77	1.8	34.93	53.67	1.65	1.07	2.44	56.12	1.28
22R-1, 91–94	903.01	1.8	35.82	55.80	1.57	1.01	2.25	55.03	1.22
22R-1, 106–110	903.16	1.8	34.75	53.25	1.63	1.07	2.39	55.42	1.24
22R-1, 126–130	903.36	1.8	37.89	61.00	1.58	0.98	2.35	58.34	1.40
22R-1, 143–147	903.53	1.8	38.00	61.30	1.57	0.97	2.33	58.20	1.39
22R-2, 6–10	903.66	1.8	38.83	63.47	1.57	0.96	2.39	59.67	1.48
22R-2, 26–30	903.86	1.8	40.44	67.91	1.51	0.90	2.24	59.77	1.49
22R-2, 45–49	904.05	1.8	40.85	69.05	1.54	0.91	2.35	61.35	1.59
22R-2, 67–71	904.27	1.8	40.61	68.37	1.53	0.91	2.32	60.75	1.55
22R-2, 81–84	904.41	1.8	40.70	68.63	1.53	0.91	2.31	60.78	1.55
22R-3, 6–10	904.50	1.8	41.28	70.31	1.52	0.90	2.32	61.48	1.60
22R-3, 24–28	904.68	1.8	37.58	60.21	1.50	0.94	2.10	55.23	1.23
22R-3, 46–50	904.90	1.8	37.96	61.17	1.58	0.98	2.36	58.47	1.41
22R-3, 66–70	905.10	1.8	36.27	56.90	1.64	1.04	2.49	58.02	1.38
22R-3, 86–90	905.30	1.8	34.92	53.66	1.64	1.07	2.43	55.99	1.27
22R-3, 106–110	905.50	1.8	34.65	53.01	1.64	1.07	2.42	55.60	1.25
22R-3, 126–130	905.70	1.8	34.46	52.58	1.64	1.08	2.41	55.27	1.24
22R-3, 146–150	905.90	1.8	35.83	55.83	1.63	1.04	2.43	56.96	1.32
22R-4, 6–10	906.00	1.8	36.13	56.57	1.62	1.04	2.43	57.27	1.34
22R-4, 26–30	906.20	1.8	35.34	54.65	1.64	1.06	2.43	56.47	1.30
22R-4, 45–49	906.39	1.8	36.82	58.27	1.60	1.01	2.37	57.46	1.35
22R-4, 63–66	906.57	1.8	34.21	51.99	1.64	1.08	2.38	54.74	1.21
22R-4, 86–89	906.80	1.8	37.59	60.24	1.60	1.00	2.41	58.65	1.42
22R-5, 6–10	907.00	1.8	38.12	61.60	1.58	0.98	2.39	59.00	1.44
22R-5, 26–30	907.20	1.8	40.15	67.09	1.55	0.93	2.36	60.71	1.55
22R-5, 45–49	907.39	1.8	39.95	66.53	1.50	0.90	2.18	58.58	1.41
22R-5, 66–70	907.60	1.8	41.28	70.31	1.53	0.90	2.34	61.65	1.61
22R-5, 84–88	907.78	1.8	41.30	70.36	1.53	0.90	2.33	61.56	1.60
22R-5, 104–108	907.98	1.8	41.82	71.88	1.54	0.89	2.40	62.73	1.68
22R-5, 123–127	908.17	1.8	40.14	67.06	1.57	0.94	2.45	61.59	1.60
22R-5, 143–147	908.37	1.8	43.77	77.85	1.48	0.83	2.27	63.29	1.72
22R-6, 6–10	908.48	1.8	45.88	84.77	1.45	0.79	2.26	65.12	1.87
22R-6, 25–29	908.67	1.8	43.02	75.51	1.48	0.85	2.25	62.38	1.66
22R-6, 46–50	908.88	1.8	42.76	74.69	1.51	0.86	2.32	62.87	1.69
22R-6, 67–71	909.09	1.8	38.53	62.67	1.56	0.96	2.31	58.57	1.41
22R-6, 86–90	909.28	1.8	39.34	64.84	1.56	0.94	2.35	59.76	1.49
22R-6, 106–110	909.48	1.8	36.03	56.32	1.60	1.02	2.34	56.29	1.29
22R-6, 116–120	909.58	1.8	33.89	51.26	1.64	1.09	2.38	54.36	1.19
22R-6, 146–150	909.88	1.8	35.16	54.23	1.63	1.06	2.41	56.03	1.27
22R-7, 6–10	909.98	1.8	33.94	51.39	1.63	1.08	2.35	54.13	1.18
22R-7, 25–29	910.17	1.8	32.17	47.43	1.69	1.15	2.46	53.22	1.14
22R-7, 49–52	910.41	1.8	34.58	52.86	1.64	1.07	2.41	55.45	1.24
22R-CC, 5–9	910.59	1.8	33.10	49.47	1.66	1.11	2.41	53.76	1.16
28R-4, 6–10	964.24	1.8	42.15	72.87	1.51	0.87	2.32	62.24	1.65
28R-4, 27–31	964.45	1.8	42.57	74.13	1.48	0.85	2.23	61.72	1.61
28R-4, 46–50	964.64	1.8	42.10	72.70	1.48	0.85	2.17	60.69	1.54
28R-4, 68–72	964.86	1.8	42.70	74.52	1.50	0.86	2.27	62.34	1.66
28R-4, 86–90	965.04	1.8	43.20	76.06	1.48	0.84	2.22	62.29	1.65
28R-4, 108–111	965.26	1.8	44.59	80.46	1.45	0.80	2.19	63.20	1.72
28R-4, 126–130	965.44	1.8	43.23	76.14	1.49	0.84	2.27	62.78	1.69
28R-4, 145–149	965.63	1.8	44.79	81.11	1.45	0.80	2.19	63.47	1.74
28R-5, 7–11	965.75	1.8	45.39	83.12	1.46	0.80	2.24	64.56	1.82
28R-5, 26–30	965.94	1.8	43.52	77.06	1.50	0.85	2.34	63.79	1.76
28R-5, 46–50	966.14	1.8	40.30	67.52	1.51	0.90	2.21	59.29	1.46
28R-5, 69–72	966.37	1.8	41.47	70.85	1.50	0.88	2.23	60.68	1.54
28R-5, 86–90	966.54	1.8	36.42	57.29	1.65	1.05	2.56	58.86	1.43
28R-5, 105–109	966.73	1.8	32.90	49.03	1.64	1.10	2.32	52.61	1.11
28R-5, 126–130	966.94	1.8	34.04	51.61	1.65	1.09	2.40	54.71	1.21
28R-5, 146–150	967.14	1.8	35.75	55.64	1.64	1.06	2.48	57.37	1.35
28R-6, 7–11	967.25	1.8	35.23	54.39	1.65	1.07	2.46	56.63	1.31
28R-6, 26–30	967.44	1.8	38.29	62.04	1.60	0.99	2.46	59.88	1.49
28R-6, 46–50	967.64	1.8	48.29	93.39	1.44	0.74	2.31	67.78	2.10

Table T2 (continued).

Core, section, interval (cm)	Depth (mbsf)	Salinity (%)	Water content		Density (g/cm ³)			Porosity (%)	Void ratio
			(% of total mass)	(% of total solids)	Bulk	Dry	Grain		
28R-6, 66–70	967.84	1.8	37.37	59.66	1.61	1.01	2.45	58.85	1.43
28R-6, 89–92	968.07	1.8	39.15	64.34	1.52	0.93	2.22	58.24	1.39
28R-6, 108–112	968.26	1.8	39.43	65.09	1.55	0.94	2.33	59.74	1.48
28R-6, 128–132	968.46	1.8	36.04	56.36	1.64	1.05	2.47	57.66	1.36
28R-CC, 0–4	968.60	1.8	35.11	54.10	1.64	1.07	2.44	56.31	1.29
29R-1, 5–9	969.55	1.8	36.15	56.61	1.61	1.03	2.37	56.74	1.31
29R-1, 28–32	969.78	1.8	36.31	57.02	1.60	1.02	2.36	56.79	1.31
29R-1, 46–50	969.96	1.8	41.01	69.51	1.53	0.90	2.32	61.19	1.58
29R-1, 71–76	970.21	1.8	42.74	74.65	1.49	0.86	2.27	62.37	1.66
29R-1, 86–90	970.36	1.8	41.56	71.12	1.53	0.89	2.36	62.06	1.64
29R-1, 106–110	970.56	1.8	42.31	73.35	1.50	0.86	2.27	61.87	1.62
29R-2, 5–9	970.72	1.8	43.23	76.14	1.49	0.84	2.26	62.70	1.68
29R-2, 23–26	970.90	1.8	45.51	83.53	1.46	0.80	2.28	65.01	1.86
29R-2, 46–50	971.13	1.8	43.76	77.80	1.47	0.83	2.24	62.96	1.70
29R-2, 68–72	971.35	1.8	43.88	78.17	1.51	0.84	2.38	64.50	1.82
29R-2, 86–90	971.53	1.8	45.57	83.71	1.46	0.79	2.25	64.81	1.84
29R-2, 106–110	971.73	1.8	45.93	84.96	1.45	0.78	2.23	64.90	1.85
29R-2, 126–131	971.93	1.8	44.56	80.39	1.47	0.81	2.24	63.76	1.76
29R-2, 144–146	972.11	1.8	43.99	78.55	1.47	0.82	2.22	63.01	1.70
29R-3, 5–9	972.18	1.8	43.87	78.15	1.47	0.83	2.25	63.15	1.71
29R-3, 30–34	972.43	1.8	41.02	69.54	1.52	0.89	2.28	60.75	1.55
29R-3, 46–50	972.59	1.8	42.39	73.58	1.49	0.86	2.25	61.82	1.62
29R-3, 66–70	972.79	1.8	44.05	78.74	1.48	0.83	2.28	63.73	1.76
29R-3, 87–91	973.00	1.8	44.05	78.73	1.48	0.83	2.30	63.88	1.77
29R-3, 113–117	973.26	1.8	44.15	79.04	1.48	0.83	2.28	63.78	1.76
29R-3, 126–130	973.39	1.8	42.48	73.85	1.50	0.86	2.27	62.12	1.64
29R-3, 146–150	973.59	1.8	39.03	64.01	1.55	0.94	2.30	59.01	1.44
29R-4, 6–10	973.69	1.8	41.76	71.69	1.51	0.88	2.29	61.61	1.60
29R-4, 26–30	973.89	1.8	40.04	66.77	1.54	0.92	2.32	60.24	1.52
29R-4, 50–54	974.13	1.8	35.15	54.21	1.60	1.04	2.31	55.02	1.22
29R-4, 65–70	974.28	1.8	39.80	66.12	1.55	0.93	2.35	60.23	1.51
29R-4, 86–90	974.49	1.8	36.11	56.52	1.62	1.03	2.40	57.01	1.33
29R-4, 106–110	974.69	1.8	36.88	58.43	1.60	1.01	2.39	57.72	1.36
29R-4, 126–130	974.89	1.8	37.01	58.75	1.59	1.00	2.37	57.63	1.36
29R-4, 144–150	975.07	1.8	36.04	56.36	1.61	1.03	2.37	56.55	1.30
29R-5, 6–10	975.19	1.8	30.95	44.83	1.70	1.18	2.43	51.49	1.06
29R-5, 24–28	975.37	1.8	35.90	56.00	1.62	1.04	2.39	56.67	1.31
29R-5, 46–50	975.59	1.8	35.11	54.10	1.62	1.05	2.36	55.48	1.25
29R-5, 66–70	975.79	1.8	37.66	60.40	1.59	0.99	2.37	58.31	1.40
29R-5, 86–90	975.99	1.8	37.74	60.62	1.58	0.99	2.37	58.38	1.40
29R-5, 110–114	976.23	1.8	35.62	55.33	1.61	1.04	2.36	56.10	1.28
29R-5, 126–130	976.39	1.8	37.24	59.35	1.59	1.00	2.38	57.96	1.38
29R-6, 6–10	976.58	1.8	38.67	63.06	1.57	0.96	2.35	59.11	1.45
29R-6, 29–34	976.81	1.8	38.72	63.18	1.55	0.95	2.30	58.62	1.42
29R-6, 46–50	976.98	1.8	41.46	70.83	1.51	0.88	2.27	61.08	1.57
29R-6, 65–70	977.17	1.8	41.58	71.18	1.51	0.88	2.29	61.37	1.59
29R-6, 86–90	977.38	1.8	43.49	76.95	1.49	0.84	2.28	63.18	1.72
29R-6, 106–110	977.58	1.8	40.71	68.67	1.53	0.91	2.32	60.86	1.55
29R-6, 126–129	977.78	1.8	41.07	69.69	1.53	0.90	2.32	61.21	1.58
29R-CC, 6–10	977.87	1.8	40.93	69.30	1.53	0.90	2.31	61.00	1.56
32R-1, 9–12	998.39	1.8	46.04	85.32	1.45	0.78	2.23	64.98	1.86
32R-1, 25–29	998.55	1.8	46.06	85.40	1.44	0.78	2.21	64.81	1.84
32R-1, 44–47	998.74	1.8	43.99	78.53	1.52	0.85	2.47	65.44	1.89
32R-1, 67–70	998.97	1.8	44.97	81.72	1.46	0.80	2.23	64.06	1.78
32R-1, 87–90	999.17	1.8	45.95	85.02	1.47	0.79	2.31	65.76	1.92
32R-1, 107–110	999.37	1.8	44.13	78.98	1.48	0.83	2.29	63.87	1.77
32R-1, 123–127	999.53	1.8	44.43	79.95	1.47	0.82	2.26	63.81	1.76
32R-2, 7–10	999.71	1.8	44.28	79.46	1.47	0.82	2.25	63.59	1.75
32R-2, 29–32	999.93	1.8	41.75	71.69	1.51	0.88	2.31	61.74	1.61
32R-2, 46–50	1000.1	1.8	43.83	78.04	1.48	0.83	2.25	63.14	1.71
32R-2, 66–70	1000.3	1.8	42.19	72.99	1.51	0.87	2.29	62.06	1.64
32R-2, 86–90	1000.5	1.8	40.63	68.44	1.60	0.95	2.60	63.46	1.74
32R-2, 106–110	1000.7	1.8	40.22	67.29	1.52	0.91	2.26	59.74	1.48
32R-2, 126–130	1000.9	1.8	39.74	65.96	1.54	0.93	2.29	59.63	1.48
32R-3, 6–10	1001.15	1.8	41.75	71.68	1.50	0.88	2.26	61.29	1.58
32R-3, 25–29	1001.34	1.8	41.51	70.98	1.51	0.88	2.26	61.04	1.57
32R-3, 47–50	1001.56	1.8	36.70	57.97	1.61	1.02	2.41	57.75	1.37
32R-3, 66–69	1001.75	1.8	36.42	57.28	1.59	1.01	2.34	56.65	1.31

Table T2 (continued).

Core, section, interval (cm)	Depth (mbsf)	Salinity (%)	Water content		Density (g/cm ³)			Porosity (%)	Void ratio
			(% of total mass)	(% of total solids)	Bulk	Dry	Grain		
32R-3, 86–90	1001.95	1.8	35.60	55.27	1.61	1.04	2.37	56.09	1.28
32R-3, 107–110	1002.16	1.8	34.23	52.05	1.64	1.08	2.39	54.89	1.22
32R-3, 126–130	1002.35	1.8	35.04	53.94	1.65	1.07	2.46	56.41	1.29
32R-3, 141–145	1002.5	1.8	31.01	44.94	1.69	1.16	2.38	51.11	1.05
32R-4, 9–13	1002.64	1.8	34.61	52.93	1.68	1.10	2.54	56.79	1.31
32R-4, 27–30	1002.82	1.8	36.05	56.37	1.31	0.83	1.54	45.95	0.85
32R-4, 47–50	1003.02	1.8	34.47	52.59	1.64	1.07	2.40	55.17	1.23
32R-4, 68–71	1003.23	1.8	34.41	52.45	1.65	1.08	2.41	55.27	1.24
32R-4, 88–91	1003.43	1.8	34.73	53.20	1.63	1.06	2.37	55.18	1.23
32R-4, 106–110	1003.61	1.8	31.57	46.13	1.69	1.16	2.42	52.12	1.09
32R-4, 126–130	1003.81	1.8	35.36	54.71	1.67	1.08	2.54	57.61	1.36
32R-4, 146–150	1004.01	1.8	33.08	49.43	1.70	1.14	2.53	54.95	1.22
32R-5, 7–10	1004.12	1.8	34.67	53.07	1.63	1.07	2.38	55.24	1.23
32R-5, 27–30	1004.32	1.8	33.18	49.65	1.66	1.11	2.40	53.77	1.16
32R-5, 47–50	1004.52	1.8	36.86	58.39	1.65	1.04	2.58	59.51	1.47
32R-5, 67–70	1004.72	1.8	38.44	62.45	1.57	0.97	2.35	58.89	1.43
32R-5, 87–90	1004.92	1.8	40.06	66.83	1.55	0.93	2.36	60.60	1.54
32R-5, 108–112	1005.13	1.8	45.20	82.50	1.46	0.80	2.25	64.40	1.81
32R-5, 125–130	1005.3	1.8	42.44	73.74	1.50	0.86	2.27	62.03	1.63
32R-5, 139–143	1005.44	1.8	43.96	78.46	1.48	0.83	2.29	63.71	1.76
32R-6, 6–9	1005.61	1.8	44.54	80.30	1.47	0.82	2.28	64.11	1.79
32R-6, 26–29	1005.81	1.8	43.19	76.04	1.49	0.84	2.26	62.65	1.68
32R-6, 47–50	1006.02	1.8	42.04	72.55	1.51	0.87	2.30	61.95	1.63
32R-6, 68–72	1006.23	1.8	43.25	76.20	1.49	0.85	2.29	63.00	1.70
32R-6, 86–89	1006.41	1.8	42.92	75.19	1.50	0.86	2.31	62.88	1.69
32R-6, 104–106	1006.59	1.8	43.85	78.09	1.51	0.85	2.39	64.55	1.82
32R-6, 124–127	1006.79	1.8	42.79	74.81	1.54	0.88	2.48	64.42	1.81
32R-6, 146–150	1007.01	1.8	44.47	80.07	1.47	0.82	2.27	63.95	1.77
32R-7, 6–9	1007.11	1.8	39.75	65.98	1.54	0.93	2.32	59.91	1.49
32R-7, 27–30	1007.32	1.8	44.22	79.27	1.47	0.82	2.24	63.40	1.73
32R-7, 46–49	1007.51	1.8	43.27	76.29	1.48	0.84	2.25	62.68	1.68
32R-CC, 7–10	1007.67	1.8	44.76	81.03	1.47	0.81	2.25	64.04	1.78
186-1151A-									
91R-1, 9–12	930.49	1.8	35.24	54.41	1.62	1.05	2.37	55.76	1.26
91R-1, 19–23	930.59	1.8	35.81	55.79	1.63	1.04	2.42	56.88	1.32
91R-1, 29–32	930.69	1.8	34.46	52.57	1.65	1.08	2.43	55.51	1.25
91R-1, 39–42	930.79	1.8	35.32	54.61	1.67	1.08	2.54	57.50	1.35
91R-1, 46–49	930.86	1.8	34.36	52.35	1.66	1.09	2.46	55.67	1.26
91R-1, 55–59	930.95	1.8	33.82	51.11	1.70	1.13	2.57	56.23	1.28
91R-1, 64–67	931.04	1.8	33.87	51.23	1.66	1.10	2.42	54.81	1.21
91R-1, 77–81	931.17	1.8	33.91	51.32	1.69	1.12	2.53	55.91	1.27
91R-1, 88–91	931.28	1.8	34.63	52.98	1.68	1.10	2.53	56.68	1.31
91R-1, 99–102	931.39	1.8	37.45	59.87	1.63	1.02	2.53	59.66	1.48
91R-1, 108–111	931.48	1.8	37.36	59.65	1.63	1.02	2.52	59.46	1.47
91R-1, 118–121	931.58	1.8	37.32	59.55	1.62	1.02	2.49	59.18	1.45
91R-1, 127–131	931.67	1.8	37.87	60.95	1.59	0.99	2.38	58.66	1.42
91R-1, 137–140	931.77	1.8	35.07	54.01	1.63	1.06	2.38	55.69	1.26
91R-1, 145–149	931.85	1.8	34.32	52.26	1.68	1.10	2.52	56.29	1.29
91R-2, 8–12	931.98	1.8	32.25	47.61	1.72	1.17	2.55	54.21	1.18
91R-2, 20–23	932.1	1.8	34.91	53.64	1.69	1.10	2.61	57.79	1.37
91R-2, 31–34	932.21	1.8	34.75	53.25	1.65	1.08	2.45	56.02	1.27
91R-2, 41–43	932.31	1.8	31.68	46.37	1.68	1.15	2.40	52.08	1.09
91R-2, 50–53	932.4	1.8	31.62	46.24	1.71	1.17	2.48	52.87	1.12
91R-2, 58–61	932.48	1.8	33.31	49.94	1.68	1.12	2.46	54.57	1.20
91R-2, 70–73	932.6	1.8	33.98	51.47	1.69	1.11	2.53	55.96	1.27
91R-2, 78–81	932.68	1.8	33.50	50.38	1.74	1.16	2.70	57.07	1.33
91R-2, 87–90	932.77	1.8	33.73	50.90	1.67	1.11	2.47	55.14	1.23
91R-2, 97–100	932.87	1.8	33.89	51.25	1.71	1.13	2.61	56.60	1.30
91R-2, 108–111	932.98	1.8	33.29	49.90	1.69	1.13	2.50	54.96	1.22
91R-2, 117–120	933.07	1.8	33.94	51.37	1.71	1.13	2.60	56.65	1.31
91R-2, 127–130	933.17	1.8	35.47	54.97	1.64	1.06	2.46	56.92	1.32
91R-2, 136–139	933.26	1.8	35.24	54.41	1.64	1.06	2.42	56.26	1.29
91R-2, 145–148	933.35	1.8	35.91	56.03	1.61	1.03	2.37	56.51	1.30
91R-3, 8–11	933.48	1.8	35.41	54.82	1.63	1.05	2.42	56.41	1.29
91R-3, 18–21	933.58	1.8	37.92	61.08	1.59	0.99	2.39	58.80	1.43
91R-3, 26–29	933.66	1.8	36.79	58.19	1.62	1.03	2.46	58.29	1.40
91R-3, 38–41	933.78	1.8	34.84	53.48	1.64	1.07	2.41	55.69	1.26
91R-3, 48–51	933.88	1.8	34.69	53.11	1.64	1.07	2.43	55.72	1.26

Table T2 (continued).

Core, section, interval (cm)	Depth (mbsf)	Salinity (%)	Water content		Density (g/cm ³)			Porosity (%)	Void ratio
			(% of total mass)	(% of total solids)	Bulk	Dry	Grain		
91R-3, 59–62	933.99	1.8	36.66	57.89	1.65	1.04	2.54	58.91	1.43
91R-3, 66–70	934.06	1.8	37.25	59.35	1.61	1.01	2.42	58.39	1.40
91R-3, 78–81	934.18	1.8	36.80	58.23	1.60	1.01	2.39	57.62	1.36
91R-3, 88–91	934.28	1.8	38.96	63.84	1.57	0.96	2.38	59.75	1.48
91R-3, 98–101	934.38	1.8	37.38	59.70	1.61	1.01	2.44	58.75	1.42
91R-3, 107–110	934.47	1.8	36.11	56.52	1.63	1.04	2.44	57.39	1.35
91R-3, 117–120	934.57	1.8	34.60	52.90	1.65	1.08	2.45	55.82	1.26
91R-3, 127–130	934.67	1.8	33.22	49.74	1.72	1.15	2.61	55.92	1.27
91R-3, 139–142	934.79	1.8	33.11	49.50	1.69	1.13	2.49	54.64	1.20
91R-3, 146–149	934.86	1.8	32.41	47.95	1.70	1.15	2.50	53.88	1.17
91R-4, 7–10	934.97	1.8	32.93	49.09	1.71	1.15	2.56	55.09	1.23
91R-4, 17–20	935.07	1.8	35.14	54.18	1.66	1.07	2.49	56.85	1.32
91R-4, 27–30	935.17	1.8	35.78	55.72	1.64	1.05	2.47	57.38	1.35
91R-4, 37–40	935.27	1.8	35.01	53.87	1.66	1.08	2.48	56.61	1.30
91R-4, 48–51	935.38	1.8	37.88	60.97	1.63	1.01	2.56	60.35	1.52
91R-4, 59–62	935.49	1.8	38.15	61.68	1.62	1.00	2.53	60.38	1.52
91R-4, 67–70	935.57	1.8	39.21	64.50	1.58	0.96	2.43	60.47	1.53
91R-4, 79–82	935.69	1.8	38.86	63.55	1.56	0.96	2.35	59.36	1.46
91R-4, 88–92	935.78	1.8	39.49	65.27	1.58	0.96	2.45	60.98	1.56
91R-4, 97–100	935.87	1.8	38.52	62.66	1.57	0.97	2.36	59.11	1.45
91R-4, 107–110	935.97	1.8	39.13	64.30	1.56	0.95	2.34	59.48	1.47
91R-4, 117–120	936.07	1.8	38.59	62.84	1.59	0.97	2.43	59.82	1.49
91R-4, 127–130	936.17	1.8	38.17	61.75	1.58	0.98	2.38	58.92	1.43
91R-4, 137–140	936.27	1.8	38.02	61.34	1.63	1.01	2.55	60.39	1.52
91R-4, 147–150	936.37	1.8	36.75	58.09	1.59	1.01	2.35	57.09	1.33
91R-5, 7–10	936.47	1.8	35.42	54.85	1.66	1.07	2.50	57.29	1.34
91R-5, 19–22	936.59	1.8	33.75	50.94	1.63	1.08	2.34	53.76	1.16
91R-5, 30–34	936.7	1.8	35.41	54.82	1.63	1.06	2.43	56.49	1.30
91R-5, 37–40	936.77	1.8	36.46	57.39	1.64	1.04	2.49	58.24	1.39
91R-5, 49–53	936.89	1.8	34.96	53.76	1.64	1.07	2.43	56.08	1.28
91R-5, 59–62	936.99	1.8	37.07	58.91	1.64	1.03	2.53	59.30	1.46
91R-5, 69–72	937.09	1.8	36.17	56.66	1.63	1.04	2.44	57.44	1.35
91R-5, 79–82	937.19	1.8	36.22	56.80	1.66	1.06	2.55	58.59	1.42
91R-5, 89–92	937.29	1.8	36.93	58.54	1.62	1.02	2.44	58.25	1.40
91R-5, 98–101	937.38	1.8	36.90	58.47	1.61	1.02	2.42	58.03	1.38
91R-5, 109–112	937.49	1.8	37.10	58.99	1.61	1.01	2.42	58.23	1.39
91R-5, 119–122	937.59	1.8	37.16	59.14	1.62	1.02	2.45	58.63	1.42
91R-5, 129–133	937.69	1.8	36.21	56.77	1.63	1.04	2.45	57.59	1.36
91R-5, 139–142	937.79	1.8	36.01	56.27	1.63	1.04	2.43	57.17	1.33
91R-5, 147–150	937.87	1.8	35.36	54.71	1.66	1.07	2.51	57.27	1.34
91R-6, 9–12	937.99	1.8	35.92	56.04	1.64	1.05	2.48	57.53	1.35
91R-6, 18–21	938.08	1.8	36.44	57.33	1.62	1.03	2.42	57.57	1.36
91R-6, 32–35	938.22	1.8	35.59	55.25	1.65	1.07	2.51	57.48	1.35
91R-6, 42–45	938.32	1.8	36.83	58.31	1.60	1.01	2.39	57.64	1.36
91R-6, 50–54	938.4	1.8	38.06	61.45	1.58	0.98	2.36	58.65	1.42
91R-6, 60–63	938.5	1.8	39.79	66.09	1.53	0.92	2.28	59.56	1.47
91R-6, 72–75	938.62	1.8	38.85	63.54	1.56	0.96	2.35	59.36	1.46
91R-6, 84–86	938.74	1.8	40.08	66.88	1.58	0.95	2.48	61.87	1.62
91R-6, 94–97	938.84	1.8	38.49	62.56	1.61	0.99	2.49	60.38	1.52
91R-6, 101–104	938.91	1.8	38.77	63.33	1.59	0.97	2.45	60.22	1.51
91R-6, 110–113	939	1.8	37.73	60.58	1.59	0.99	2.38	58.43	1.41
91R-6, 119–122	939.09	1.8	34.95	53.72	1.63	1.06	2.40	55.76	1.26
91R-6, 128–131	939.18	1.8	35.82	55.82	1.60	1.03	2.33	55.92	1.27
91R-6, 137–140	939.27	1.8	34.68	53.08	1.62	1.06	2.35	54.88	1.22
91R-CC, 6–9	939.39	1.8	34.25	52.08	1.64	1.08	2.40	54.98	1.22
91R-CC, 18–21	939.51	1.8	34.29	52.19	1.68	1.10	2.52	56.23	1.28
105R-1, 6–9	1065.36	1.8	35.35	54.68	1.60	1.03	2.30	55.10	1.23
105R-1, 18–21	1065.48	1.8	36.17	56.67	1.58	1.01	2.28	55.74	1.26
105R-1, 28–31	1065.58	1.8	36.55	57.61	1.54	0.98	2.18	55.12	1.23
105R-1, 38–41	1065.68	1.8	34.53	52.75	1.62	1.06	2.34	54.70	1.21
105R-1, 49–51	1065.79	1.8	36.13	56.56	1.56	1.00	2.22	55.07	1.23
105R-1, 56–60	1065.86	1.8	36.43	57.32	1.39	0.88	1.74	49.33	0.97
105R-1, 69–72	1065.99	1.8	36.16	56.65	1.55	0.99	2.18	54.67	1.21
105R-1, 79–82	1066.09	1.8	36.33	57.06	1.76	1.12	2.97	62.33	1.65
105R-1, 88–91	1066.18	1.8	35.86	55.90	1.48	0.95	1.97	51.87	1.08
105R-1, 97–100	1066.27	1.8	36.06	56.39	1.56	1.00	2.22	54.97	1.22
105R-1, 110–112	1066.4	1.8	35.19	54.30	1.63	1.06	2.41	56.14	1.28
105R-1, 119–122	1066.49	1.8	36.46	57.39	1.62	1.03	2.44	57.77	1.37

Table T2 (continued).

Core, section, interval (cm)	Depth (mbsf)	Salinity (%)	Water content		Density (g/cm ³)			Porosity (%)	Void ratio
			(% of total mass)	(% of total solids)	Bulk	Dry	Grain		
105R-1, 130–133	1066.6	1.8	35.81	55.79	1.61	1.03	2.35	56.19	1.28
105R-1, 137–140	1066.67	1.8	36.36	57.14	1.71	1.09	2.75	60.57	1.54
105R-1, 146–149	1066.76	1.8	34.67	53.08	1.58	1.03	2.23	53.59	1.15
105R-2, 8–11	1066.88	1.8	36.02	56.30	1.68	1.08	2.63	59.11	1.45
105R-2, 17–20	1066.97	1.8	35.94	56.11	1.56	1.00	2.21	54.73	1.21
105R-2, 27–30	1067.07	1.8	35.66	55.43	1.62	1.04	2.39	56.41	1.29
105R-2, 37–40	1067.17	1.8	35.24	54.41	1.72	1.11	2.72	59.11	1.45
105R-2, 46–49	1067.26	1.8	35.11	54.10	1.64	1.06	2.42	56.08	1.28
105R-2, 57–60	1067.37	1.8	35.89	55.98	1.58	1.01	2.26	55.22	1.23
105R-2, 67–70	1067.47	1.8	35.44	54.89	1.69	1.09	2.63	58.53	1.41
105R-2, 77–80	1067.57	1.8	35.39	54.78	1.60	1.03	2.31	55.32	1.24
105R-2, 87–89	1067.67	1.8	34.83	53.44	1.76	1.14	2.84	59.73	1.48
105R-2, 97–100	1067.77	1.8	34.26	52.11	1.66	1.09	2.45	55.51	1.25
105R-2, 107–110	1067.87	1.8	34.41	52.46	1.60	1.05	2.28	53.83	1.17
105R-2, 117–120	1067.97	1.8	34.08	51.70	1.61	1.06	2.28	53.49	1.15
105R-2, 130–133	1068.1	1.8	34.40	52.44	1.63	1.07	2.36	54.74	1.21
105R-2, 137–140	1068.17	1.8	34.47	52.60	1.62	1.06	2.35	54.67	1.21
105R-2, 147–149	1068.27	1.8	35.10	54.09	1.56	1.01	2.19	53.58	1.15
105R-3, 7–10	1068.37	1.8	36.29	56.96	1.58	1.01	2.28	55.93	1.27
105R-3, 18–21	1068.48	1.8	35.01	53.87	1.59	1.03	2.26	54.30	1.19
105R-3, 26–29	1068.56	1.8	31.85	46.73	1.76	1.20	2.64	54.62	1.20
105R-3, 38–41	1068.68	1.8	36.07	56.41	1.69	1.08	2.68	59.61	1.48
105R-3, 50–52	1068.8	1.8	35.89	55.99	1.54	0.99	2.15	54.07	1.18
105R-3, 58–61	1068.88	1.8	35.64	55.38	1.63	1.05	2.41	56.63	1.31
105R-3, 68–70	1068.98	1.8	35.45	54.92	1.62	1.05	2.40	56.25	1.29
105R-3, 79–82	1069.09	1.8	32.79	48.78	1.64	1.10	2.33	52.59	1.11
105R-3, 87–90	1069.17	1.8	34.94	53.70	1.62	1.05	2.34	55.13	1.23
105R-3, 97–100	1069.27	1.8	34.71	53.15	1.73	1.13	2.72	58.53	1.41
105R-3, 105–107	1069.35	1.8	33.73	50.90	1.64	1.09	2.36	53.99	1.17
105R-3, 115–118	1069.45	1.8	33.80	51.05	1.59	1.05	2.21	52.42	1.10
105R-3, 126–129	1069.56	1.8	35.03	53.91	1.70	1.10	2.63	58.11	1.39
105R-3, 138–141	1069.68	1.8	36.67	57.89	1.60	1.01	2.37	57.23	1.34
105R-3, 147–150	1069.77	1.8	33.72	50.88	1.69	1.12	2.51	55.54	1.25
105R-4, 7–10	1069.88	1.8	33.59	50.58	1.60	1.06	2.23	52.46	1.10
105R-4, 16–18	1069.97	1.8	33.91	51.31	1.76	1.16	2.77	58.13	1.39
105R-4, 26–29	1070.07	1.8	33.23	49.76	1.73	1.15	2.62	55.98	1.27
105R-4, 36–39	1070.17	1.8	34.49	52.64	1.62	1.06	2.35	54.66	1.21
105R-4, 47–50	1070.28	1.8	33.51	50.40	1.64	1.09	2.34	53.51	1.15
105R-4, 56–59	1070.37	1.8	33.84	51.15	1.62	1.07	2.32	53.69	1.16
105R-4, 64–67	1070.45	1.8	32.71	48.61	1.74	1.17	2.62	55.45	1.24
105R-4, 78–81	1070.59	1.8	34.99	53.83	1.62	1.05	2.35	55.26	1.24
105R-4, 87–90	1070.68	1.8	32.38	47.88	1.64	1.11	2.32	52.00	1.08
105R-4, 96–99	1070.77	1.8	33.38	50.11	1.62	1.08	2.27	52.65	1.11
105R-4, 107–110	1070.88	1.8	33.57	50.54	1.66	1.10	2.41	54.35	1.19
105R-4, 117–120	1070.98	1.8	35.00	53.85	1.64	1.07	2.43	56.10	1.28
105R-4, 130–133	1071.11	1.8	34.53	52.74	1.72	1.13	2.69	58.11	1.39
105R-4, 138–141	1071.19	1.8	34.89	53.58	1.56	1.02	2.17	53.15	1.13
105R-4, 147–150	1071.28	1.8	33.36	50.05	1.67	1.11	2.43	54.25	1.19
105R-5, 7–10	1071.38	1.8	35.80	55.75	1.58	1.01	2.26	55.20	1.23
105R-5, 17–20	1071.48	1.8	35.91	56.03	1.61	1.03	2.38	56.56	1.30
105R-5, 28–30	1071.59	1.8	35.41	54.83	1.61	1.04	2.35	55.74	1.26
105R-5, 35–39	1071.66	1.8	32.08	47.24	1.73	1.18	2.57	54.23	1.18
105R-5, 49–52	1071.8	1.8	37.63	60.34	1.58	0.98	2.34	57.92	1.38
105R-5, 57–60	1071.88	1.8	38.03	61.37	1.56	0.97	2.31	58.02	1.38
105R-5, 69–73	1072	1.8	35.28	54.52	1.63	1.06	2.41	56.20	1.28
105R-5, 77–80	1072.08	1.8	35.96	56.16	1.57	1.01	2.24	55.18	1.23
105R-5, 87–90	1072.18	1.8	35.38	54.75	1.69	1.10	2.64	58.54	1.41
105R-5, 97–100	1072.28	1.8	36.50	57.48	1.58	1.00	2.29	56.29	1.29
105R-5, 107–110	1072.38	1.8	34.58	52.86	1.70	1.11	2.62	57.49	1.35
105R-5, 118–122	1072.49	1.8	36.61	57.76	1.57	0.99	2.26	56.02	1.27
105R-5, 127–130	1072.58	1.8	35.56	55.18	1.60	1.03	2.32	55.59	1.25
105R-5, 137–140	1072.68	1.8	34.24	52.07	1.74	1.14	2.73	58.14	1.39
105R-5, 147–150	1072.78	1.8	33.84	51.14	1.67	1.10	2.46	55.16	1.23
105R-6, 8–12	1072.89	1.8	37.07	58.89	1.54	0.97	2.19	55.73	1.26
105R-6, 17–20	1072.98	1.8	36.80	58.22	1.60	1.01	2.37	57.43	1.35
105R-6, 27–30	1073.08	1.8	36.40	57.23	1.67	1.06	2.63	59.46	1.47
105R-6, 37–40	1073.18	1.8	35.84	55.87	1.66	1.06	2.52	57.93	1.38
105R-6, 47–50	1073.28	1.8	36.10	56.51	1.64	1.04	2.47	57.65	1.36

Table T2 (continued).

Core, section, interval (cm)	Depth (mbsf)	Salinity (%)	Water content		Density (g/cm ³)			Porosity (%)	Void ratio
			(% of total mass)	(% of total solids)	Bulk	Dry	Grain		
105R-6, 60–63	1073.41	1.8	36.10	56.50	1.57	1.00	2.24	55.31	1.24
105R-6, 67–70	1073.48	1.8	38.19	61.78	1.61	1.00	2.50	60.10	1.51
105R-6, 78–81	1073.59	1.8	38.02	61.35	1.37	0.85	1.72	50.71	1.03
105R-6, 87–90	1073.68	1.8	36.63	57.80	1.57	1.00	2.27	56.19	1.28
105R-6, 99–102	1073.8	1.8	36.83	58.31	1.65	1.04	2.58	59.46	1.47
105R-6, 107–110	1073.88	1.8	37.12	59.04	1.63	1.02	2.50	59.08	1.44
105R-6, 117–120	1073.98	1.8	36.46	57.38	1.69	1.07	2.69	60.09	1.51
105R-6, 127–130	1074.08	1.8	37.98	61.25	1.62	1.01	2.53	60.17	1.51
105R-6, 137–140	1074.18	1.8	38.69	63.10	1.51	0.93	2.16	57.05	1.33
105R-CC, 6–9	1074.31	1.8	36.37	57.15	1.68	1.07	2.64	59.58	1.47
105R-CC, 15–18	1074.4	1.8	37.44	59.85	1.65	1.03	2.61	60.37	1.52

Table T3. Results of diatom analysis and TOC analyses for selected samples, Sites 1150 and 1151. (See table notes. Continued on next page.)

Core, section, interval (cm)	Depth (mbsf)	Diatom valves			TOC (wt%)		Diatom valves			TOC (wt%)	
		Counted number/g	Absolute number/g				Counted number/g	Absolute number/g			
186-1150B-											
22R-1, 8–12	902.18	456	1.9018E+08	0.570			32R-2, 86–90	1000.50	113	4.7920E+07	ND
22R-1, 46–50	902.56	265	1.2102E+08	0.478			32R-2, 106–110	1000.70	82	3.3372E+07	0.656
22R-1, 91–94	903.01	202	7.0302E+07	0.552			32R-2, 126–130	1000.90	84	3.0942E+07	ND
22R-1, 126–130	903.36	326	1.3430E+08	1.037			32R-3, 6–10	1001.15	107	4.9767E+07	0.571
22R-2, 6–10	903.66	265	1.2325E+08	0.450			32R-3, 47–50	1001.56	79	3.6575E+07	0.598
22R-2, 45–49	904.05	ND	ND	0.403			32R-3, 66–69	1001.75	108	4.4310E+07	ND
22R-2, 81–84	904.41	454	1.6602E+08	0.317			32R-3, 86–90	1001.95	126	6.2034E+07	0.649
22R-3, 24–28	904.68	206	9.8072E+07	0.314			32R-3, 126–130	1002.35	99	4.4017E+07	0.693
22R-3, 66–70	905.10	180	7.5071E+07	0.527			32R-4, 9–13	1002.64	105	3.8397E+07	0.754
22R-3, 106–110	905.50	ND	ND	0.404			32R-4, 47–50	1003.02	121	5.4277E+07	0.623
22R-3, 146–150	905.90	221	8.3228E+07	0.434			32R-4, 88–91	1003.43	123	5.3975E+07	0.709
22R-4, 26–30	906.20	161	7.0344E+07	0.331			32R-4, 126–130	1003.81	93	4.2665E+07	0.622
22R-4, 63–66	906.57	264	1.1102E+08	0.390			32R-5, 7–10	1004.12	85	4.2054E+07	0.719
22R-5, 6–10	907.00	286	1.3489E+08	0.661			32R-5, 47–50	1004.52	79	3.2022E+07	0.792
22R-5, 45–49	907.39	329	1.4957E+08	0.470			32R-5, 87–90	1004.92	159	6.7999E+07	0.710
22R-5, 84–88	907.78	363	1.7120E+08	0.326			32R-5, 125–130	1005.30	ND	ND	0.682
22R-5, 123–127	908.17	336	1.4874E+08	0.337			32R-6, 6–9	1005.61	155	7.1109E+07	0.600
22R-6, 6–10	908.48	354	1.7344E+08	0.325			32R-6, 47–50	1006.02	133	4.5658E+07	0.598
22R-6, 46–50	908.88	255	8.6365E+07	0.311			32R-6, 86–89	1006.41	92	3.9681E+07	0.675
22R-6, 86–90	909.28	254	1.0254E+08	0.300			32R-6, 124–127	1006.79	119	5.8303E+07	0.674
22R-6, 116–120	909.58	52	2.3856E+07	0.344			32R-7, 6–9	1007.11	122	5.4726E+07	0.567
22R-7, 6–10	909.98	190	7.8271E+07	0.545			32R-7, 46–49	1007.51	151	6.5129E+07	0.665
22R-7, 49–52	910.41	254	1.0817E+08	0.235			32R-CC, 7–10	1007.67	ND	ND	0.766
22R-CC, 5–9	910.59	ND	ND	0.195							
28R-4, 6–10	964.24	326	1.6129E+08	0.228		186-1151A-					
28R-4, 46–50	964.64	244	1.0218E+08	0.208		105R-1, 6–9	1065.36	102	6.5571E+07	0.390	
28R-4, 86–90	965.04	265	1.2213E+08	0.390		105R-1, 18–21	1065.48	137	7.9926E+07	ND	
28R-4, 126–130	965.44	311	1.1131E+08	0.880		105R-1, 28–31	1065.58	91	5.4997E+07	0.218	
28R-5, 7–11	965.75	249	1.0052E+08	0.893		105R-1, 38–41	1065.68	112	6.6494E+07	ND	
28R-5, 46–50	966.14	243	9.8497E+07	0.236		105R-1, 49–51	1065.79	119	7.3235E+07	0.405	
28R-5, 86–90	966.54	161	7.1900E+07	0.321		105R-1, 56–60	1065.86	101	6.6626E+07	ND	
28R-5, 126–130	966.94	ND	ND	0.321		105R-1, 69–72	1065.99	135	7.9680E+07	0.270	
28R-6, 7–11	967.25	160	6.6730E+07	0.268		105R-1, 79–82	1066.09	70	4.1559E+07	ND	
28R-6, 46–50	967.64	349	1.6158E+08	0.815		105R-1, 88–91	1066.18	122	6.9962E+07	0.225	
28R-6, 89–92	968.07	340	1.6187E+08	0.688		105R-1, 97–100	1066.27	119	6.8241E+07	ND	
28R-6, 128–132	968.46	308	1.4066E+08	0.655		105R-1, 110–112	1066.40	81	4.3255E+07	0.229	
29R-1, 5–9	969.55	154	9.1429E+07	0.589		105R-1, 119–122	1066.49	78	4.2785E+07	ND	
29R-1, 46–50	969.96	177	1.0960E+08	0.744		105R-1, 130–133	1066.60	99	4.9960E+07	0.309	
29R-1, 86–90	970.36	185	1.1893E+08	0.806		105R-1, 137–140	1066.67	88	5.0179E+07	ND	
29R-2, 5–9	970.72	217	1.2733E+08	0.776		105R-1, 146–149	1066.76	131	7.4699E+07	0.291	
29R-2, 46–50	971.13	166	1.0154E+08	0.685		105R-2, 8–11	1066.88	114	6.0240E+07	ND	
29R-2, 86–90	971.53	164	9.0947E+07	0.792		105R-2, 17–20	1066.97	70	4.3882E+07	0.269	
29R-2, 126–131	971.93	163	9.2423E+07	ND		105R-2, 27–30	1067.07	95	5.5423E+07	ND	
29R-3, 5–9	972.18	ND	ND	0.694		105R-2, 37–40	1067.17	98	6.1435E+07	0.308	
29R-3, 46–50	972.59	147	8.3351E+07	0.701		105R-2, 46–49	1067.26	109	5.6707E+07	ND	
29R-3, 87–91	973.00	191	1.1827E+08	0.690		105R-2, 57–60	1067.37	80	4.6139E+07	0.224	
29R-3, 126–130	973.39	211	1.3227E+08	0.702		105R-2, 67–70	1067.47	115	6.9920E+07	ND	
29R-4, 6–10	973.69	121	7.7786E+07	0.786		105R-2, 77–80	1067.57	62	3.8627E+07	0.269	
29R-4, 50–54	974.13	115	5.5008E+07	0.584		105R-2, 87–89	1067.67	55	3.4912E+07	ND	
29R-4, 86–90	974.49	150	8.6510E+07	0.655		105R-2, 97–100	1067.77	83	4.2523E+07	0.252	
29R-4, 126–130	974.89	178	8.1660E+07	0.683		105R-2, 107–110	1067.87	122	6.9176E+07	ND	
29R-5, 6–10	975.19	94	5.4525E+07	0.534		105R-2, 117–120	1067.97	98	5.3177E+07	0.220	
29R-5, 46–50	975.59	139	7.2690E+07	0.748		105R-2, 130–133	1068.10	71	4.2402E+07	ND	
29R-5, 86–90	975.99	180	1.1010E+08	0.704		105R-2, 137–140	1068.17	109	6.7909E+07	0.287	
29R-5, 126–130	976.39	194	1.2238E+08	0.725		105R-2, 147–149	1068.27	140	8.3609E+07	ND	
29R-6, 29–34	976.81	101	5.8250E+07	0.842		105R-3, 7–10	1068.37	95	5.4479E+07	0.252	
29R-6, 65–70	977.17	119	7.1919E+07	0.814		105R-3, 18–21	1068.48	131	6.8153E+07	ND	
29R-6, 106–110	977.58	120	7.2960E+07	0.761		105R-3, 26–29	1068.56	59	3.3454E+07	0.208	
29R-CC, 6–10	977.87	213	1.3108E+08	0.735		105R-3, 38–41	1068.68	96	5.6332E+07	ND	
32R-1, 9–12	998.39	159	7.4989E+07	0.703		105R-3, 50–52	1068.80	76	4.4857E+07	0.303	
32R-1, 44–47	998.74	110	4.6452E+07	0.686		105R-3, 58–61	1068.88	101	5.9613E+07	ND	
32R-1, 87–90	999.17	81	3.7674E+07	0.833		105R-3, 68–70	1068.98	101	5.7592E+07	0.135	
32R-1, 123–127	999.53	75	3.6746E+07	0.902		105R-3, 79–82	1069.09	81	4.9547E+07	ND	
32R-2, 29–32	999.93	56	2.7304E+07	0.607		105R-3, 87–90	1069.17	105	5.3254E+07	0.225	
32R-2, 66–70	1000.30	105	5.0950E+07	0.699		105R-3, 97–100	1069.27	117	7.2004E+07	ND	
						105R-3, 105–107	1069.35	77	4.8572E+07	0.221	
						105R-3, 115–118	1069.45	83	5.4046E+07	ND	
						105R-3, 126–129	1069.56	85	5.6071E+07	0.179	

Table T3 (continued).

Core, section, interval (cm)	Depth (mbsf)	Diatom valves		
		Counted number/g	Absolute number/g	TOC (wt%)
105R-3, 138–141	1069.68	126	6.6932E+07	ND
105R-3, 147–150	1069.77	108	6.0895E+07	0.186
105R-4, 7–10	1069.88	101	5.5401E+07	ND
105R-4, 16–18	1069.97	81	4.5167E+07	0.188
105R-4, 26–29	1070.07	68	3.9902E+07	0.151
105R-4, 47–50	1070.28	81	5.0464E+07	0.174
105R-4, 56–59	1070.37	45	2.8210E+07	ND
105R-4, 64–67	1070.45	53	2.9231E+07	ND
105R-4, 78–81	1070.59	81	4.4431E+07	0.290
105R-4, 87–90	1070.68	82	4.3331E+07	ND
105R-4, 96–99	1070.77	58	3.3837E+07	ND
105R-4, 107–110	1070.88	88	4.7751E+07	0.268
105R-4, 117–120	1070.98	66	3.8505E+07	ND
105R-4, 130–133	1071.11	59	3.5445E+07	0.223
105R-4, 138–141	1071.19	65	3.9050E+07	ND
105R-4, 147–150	1071.28	68	3.5746E+07	0.257
105R-5, 17–20	1071.48	82	4.9856E+07	0.221
105R-5, 28–30	1071.59	49	3.1301E+07	ND
105R-5, 35–39	1071.66	43	2.1809E+07	0.187
105R-5, 49–52	1071.80	112	5.9495E+07	ND
105R-5, 57–60	1071.88	125	6.8940E+07	0.260
105R-5, 69–73	1072.00	94	5.5808E+07	ND
105R-5, 77–80	1072.08	73	3.9612E+07	0.171
105R-5, 87–90	1072.18	63	3.7624E+07	ND
105R-5, 97–100	1072.28	63	3.6128E+07	0.187
105R-5, 107–110	1072.38	49	3.1500E+07	ND
105R-5, 118–122	1072.49	85	5.2956E+07	0.160
105R-5, 127–130	1072.58	94	5.0197E+07	ND
105R-5, 137–140	1072.68	113	6.1983E+07	0.203
105R-5, 147–150	1072.78	49	2.7025E+07	ND
105R-6, 8–12	1072.89	79	4.5047E+07	0.347
105R-6, 17–20	1072.98	101	6.2157E+07	ND
105R-6, 27–30	1073.08	218	1.3666E+08	0.238
105R-6, 37–40	1073.18	166	9.9727E+07	ND
105R-6, 47–50	1073.28	178	1.0822E+08	0.205
105R-6, 60–63	1073.41	134	7.5980E+07	ND
105R-6, 67–70	1073.48	207	1.2977E+08	0.223
105R-6, 78–81	1073.59	280	1.7127E+08	ND
105R-6, 87–90	1073.68	313	1.8917E+08	0.175
105R-6, 107–110	1073.88	262	1.5834E+08	0.288
105R-6, 117–120	1073.98	273	1.4894E+08	ND
105R-6, 127–130	1074.08	274	1.6461E+08	0.258
105R-6, 137–140	1074.18	357	2.1706E+08	ND
105R-CC, 6–9	1074.31	298	1.7187E+08	0.283
105R-CC, 15–18	1074.40	192	1.1962E+08	ND

Notes: ND = no data. TOC = total organic carbon.

Table T4. Depth of tie points and depth offsets in recovered cores from Holes 1150A and 1150B with logging depths, Hole 1150D.

Depth of recovered core (mbsf)	Logging depth (mbsf)	Offset (m)	Depth of recovered core (mbsf)	Logging depth (mbsf)	Offset (m)	Depth of recovered core (mbsf)	Logging depth (mbsf)	Offset (m)
186-1150A-	186-1150D-		447.6	Tie to 452.3	-4.7	947.8	Tie to 951.0	-3.1
117.7	Tie to 121.0	-3.3	462.1	Tie to 466.2	-4.1	950.4	Tie to 952.0	-1.7
127.6	Tie to 132.3	-4.7	502.0	Tie to 506.1	-4.1	957.3	Tie to 959.8	-2.5
129.3	Tie to 133.8	-4.5	509.7	Tie to 513.3	-3.6	960.0	Tie to 961.6	-1.7
136.1	Tie to 138.4	-2.3	518.4	Tie to 520.1	-1.8	968.5	Tie to 970.3	-1.9
138.4	Tie to 140.7	-2.3	186-1150B-			969.6	Tie to 971.1	-1.5
145.9	Tie to 144.9	0.9	729.1	Tie to 732.0	-2.9	976.4	Tie to 977.6	-1.2
148.0	Tie to 148.3	-0.3	732.2	Tie to 735.0	-2.8	979.2	Tie to 979.6	-0.4
153.6	Tie to 153.2	0.4	738.7	Tie to 743.7	-5.0	983.5	Tie to 984.7	-1.2
155.7	Tie to 155.8	-0.1	739.7	Tie to 745.1	-5.4	987.5	Tie to 989.7	-2.2
158.9	Tie to 159.3	-0.4	748.4	Tie to 748.4	0	988.8	Tie to 992.1	-3.3
160.4	Tie to 161.4	-1.0	756.1	Tie to 754.8	1.3	992.0	Tie to 999.0	-7.0
184.5	Tie to 185.3	-0.8	758.0	Tie to 757.1	0.9	998.4	Tie to 1000.0	-1.6
186.0	Tie to 186.5	-0.6	759.2	Tie to 758.3	0.8	1002.2	Tie to 1004.0	-1.8
188.4	Tie to 188.7	-0.3	767.7	Tie to 767.8	-0.1	1007.3	Tie to 1008.9	-1.6
191.2	Tie to 191.4	-0.2	769.8	Tie to 770.8	-1.1	1008.0	Tie to 1010.7	-2.7
198.3	Tie to 200.3	-2.0	777.3	Tie to 779.1	-1.8	1009.2	Tie to 1012.7	-3.5
200.0	Tie to 202.1	-2.1	781.1	Tie to 783.3	-2.3	1017.6	Tie to 1018.6	-1.0
202.1	Tie to 207.0	-4.9	787.0	Tie to 787.1	-0.2	1019.7	Tie to 1021.2	-1.5
206.7	Tie to 212.6	-5.8	790.7	Tie to 792.9	-2.2	1027.2	Tie to 1027.6	-0.4
213.0	Tie to 217.6	-4.6	796.6	Tie to 796.9	-0.3	1031.4	Tie to 1032.0	-0.6
222.3	Tie to 225.1	-2.8	802.5	Tie to 804.2	-1.7	1036.8	Tie to 1037.2	-0.4
232.2	Tie to 232.1	0.1	806.2	Tie to 805.9	0.3	1044.3	Tie to 1045.3	-1.0
234.7	Tie to 238.2	-3.5	808.6	Tie to 809.1	-0.5	1046.6	Tie to 1046.7	-0.1
239.2	Tie to 242.8	-3.6	810.5	Tie to 812.3	-1.8	1050.1	Tie to 1050.9	-0.8
241.6	Tie to 243.7	-2.1	811.7	Tie to 814.1	-2.5	1056.4	Tie to 1056.6	-0.2
244.1	Tie to 247.5	-3.4	815.8	Tie to 818.1	-2.3	1058.3	Tie to 1058.4	-0.1
252.3	Tie to 254.0	-1.8	819.5	Tie to 821.3	-1.8	1066.1	Tie to 1066.3	-0.2
261.3	Tie to 264.0	-2.7	825.5	Tie to 826.6	-1.1	1070.4	Tie to 1070.9	-0.5
272.8	Tie to 274.0	-1.2	830.4	Tie to 832.4	-2.0	1075.8	Tie to 1076.7	-0.9
276.9	Tie to 279.7	-2.8	844.7	Tie to 845.4	-0.7	1078.7	Tie to 1080.5	-1.8
281.7	Tie to 283.9	-2.3	851.7	Tie to 853.1	-1.5	1085.4	Tie to 1086.3	-0.9
292.1	Tie to 295.5	-3.4	854.3	Tie to 855.7	-1.4	1087.4	Tie to 1088.6	-1.2
296.0	Tie to 300.8	-4.8	859.4	Tie to 861.4	-2.0	1089.8	Tie to 1091.5	-1.7
309.2	Tie to 310.4	-1.3	863.9	Tie to 863.8	0.1	1094.0	Tie to 1094.7	-0.7
315.6	Tie to 316.8	-1.3	867.7	Tie to 869.0	-1.3	1095.0	Tie to 1095.7	-0.7
318.5	Tie to 320.6	-2.2	873.6	Tie to 874.6	-1.0	1096.0	Tie to 1097.4	-1.4
329.5	Tie to 329.6	-0.1	877.2	Tie to 879.5	-2.3	1096.9	Tie to 1098.6	-1.7
337.8	Tie to 337.3	0.5	883.3	Tie to 884.2	-0.9	1098.0	Tie to 1099.7	-1.7
344.9	Tie to 344.3	0.6	890.4	Tie to 890.2	0.2	1099.7	Tie to 1101.2	-1.5
350.2	Tie to 351.7	-1.6	890.7	Tie to 892.1	-1.5	1103.5	Tie to 1104.1	-0.6
360.3	Tie to 360.9	-0.6	898.1	Tie to 899.8	-1.7	1104.7	Tie to 1105.7	-1.0
365.2	Tie to 367.1	-1.9	902.2	Tie to 901.4	0.7	1111.0	Tie to 1114.2	-3.2
366.3	Tie to 368.7	-2.4	905.1	Tie to 906.0	-0.9	1114.3	Tie to 1117.5	-3.2
367.3	Tie to 369.9	-2.6	906.6	Tie to 907.2	-0.6	1114.7	Tie to 1118.3	-3.6
368.8	Tie to 371.1	-2.3	909.1	Tie to 909.7	-0.6	1115.5	Tie to 1118.9	-3.4
373.9	Tie to 376.4	-2.5	909.7	Tie to 911.0	-1.3	1124.0	Tie to 1124.4	-0.4
394.6	Tie to 396.7	-2.1	910.4	Tie to 912.0	-1.6	1128.0	Tie to 1127.4	0.6
407.0	Tie to 409.5	-2.5	911.9	Tie to 912.7	-0.8	1129.5	Tie to 1129.9	-0.4
414.9	Tie to 415.7	-0.9	919.3	Tie to 920.3	-1.1	1133.6	Tie to 1134.8	-1.2
418.7	Tie to 423.5	-4.8	921.6	Tie to 921.9	-0.3	1136.1	Tie to 1137.8	-1.7
424.5	Tie to 427.6	-3.1	923.4	Tie to 923.7	-0.3	1137.4	Tie to 1139.0	-1.6
427.8	Tie to 435.4	-7.6	931.2	Tie to 932.7	-1.5	1138.7	Tie to 1140.6	-1.9
435.2	Tie to 439.7	-4.5	938.9	Tie to 940.5	-1.6	1143.2	Tie to 1144.1	-0.9
436.7	Tie to 442.0	-5.3	940.8	Tie to 941.7	-0.9	1145.7	Tie to 1146.5	-0.8
440.8	Tie to 447.7	-7.0				1146.9	Tie to 1148.0	-1.1

Table T5. Stratigraphic events used in this study to transfer depth series of natural gamma ray intensity to time series.

Stratigraphic event	Age (Ma)	Core, section, interval (cm)	Depth (mbsf)	Middle depth (mbsf)
		186-1150A-	23.95/26.95	25.45
FO <i>Emiliania huxleyi</i>	0.248	3H-5, 75-76/3H-7, 75-76	46.33/55.73	51.03
LO <i>Proboscia curvirostris</i>	0.30	5H-CC/6H-CC	69.65/76.15	72.90
LO <i>Stylatractus universus</i>	0.43	8H-4, 45-47/9H-2, 45-47	72.61/73.21	72.91
B C1n (B Brunhes)	0.780	8H-6, 41/8H-6, 100	92.46/93.96	93.21
FO <i>Gephyrocapsa parallela</i>	0.940	10H-7, 75-76/11H-1, 76-77	95.16/98.16	96.66
LO <i>Eucyrtidium matuyamai</i>	1.03	11H-2, 46-48/11H-4, 46-48	124.7/126.8	125.75
FO <i>Gephyrocapsa caribbeanica</i>	1.71	14X-CC/15H-1, 75-76	122.82/136	129.41
LO <i>Neogloboquadrina asanoi</i>	1.8	14X-5, 42-44/16X-1, 40-44	139.36/139.6	139.48
LO <i>Discoaster brouweri</i>	1.95	16X-3, 76-77/16X-CC	184.6/185.1	184.85
T C2An (T Gauss)	2.581	21X-1, 100/21X-2, 92	250.6/251.2	250.90
LO <i>Discoaster tamalis</i>	2.82	27X-7, 10/11/27X-CC	313.14/314.73	313.94
T C3n.1n (T Cochiti)	4.180	34X-3, 103/34X-4, 112	428.66/434.31	431.49
B C3n.1n (B Cochiti)	4.290	46X-3, 135/47X-1, 21	626.08/626.74	626.41
T C3n.3n (T Sidufjall)	4.800	66X-6, 128/66X-7, 43	681.69/682.57	682.13
B C3n.3n (B Sidufjall)	4.890	72X-5, 142/72X-6, 67	723/729.41	726.21
T C3n.4n (T Thvera)	4.980	76X-7, 99/B-4R-1, 41		
		186-1150B-		
FO <i>Spongurus pylomaticus</i>	5.2	10R-2, 45-47/11R-2, 45-47	788.85/798.45	793.65
RD <i>Lithelius barbatus</i>	5.3	10R-2, 45-47/11R-2, 45-47	788.85/798.45	793.65
LO <i>Lychnocanoma parallelipes</i>	5.6	18R-2, 51-53/19R-2, 44-46	865.81/875.44	870.63
FO <i>Lychnocanoma parallelipes</i>	7.3	22R-CC/23R-CC	910.67/919.73	915.20
LCO <i>Thalassionema schraderi</i>	7.6	35R-CC/36R-CC	1031.5/1044.7	1038
FO <i>Discoaster berggrenii</i>	8.281	38R-CC/39R-1, 10-11	1058.6/1066.1	1062
LCO <i>Denticulopsis simonsenii</i>	8.6	40R-CC/41R-1, 68-71	1079.21/1085.93	1083
LO <i>Denticulopsis dimorpha</i>	9.16	43R-1, 69-71/43R-3, 71-72	1105.29/1108.26	1107
FO <i>Denticulopsis dimorpha</i>	9.9	48R-CC/49R-CC	1157.71/1170.57	1164
LCO <i>Denticulopsis praedimorpha</i>	11.5	Below 50R-CC	1180	1180

Notes: LO = last occurrence, FO = first occurrence, FCO = first common occurrence, LCO = last common occurrence. RI = rapid increase, RD = rapid decrease. T = top of chron, B = bottom of chron. Slash = between.

Table T6. List of low and high sedimentation rate stages in variation of the NGR intensity.

Stage	Age (Ma)		Sedimentation rate (cm/k.y.)	Measured data		Resampled data		Intensity of power spectrum density		
	Top	Bottom		N	Δt (Ma)	N	Δt (Ma)	Eccentricity	Obliquity	Precession
L1	1.32	2.58	6	479	0.0026	315	0.0040	High	High	Low
H1	2.58	2.82	28	442	0.0005	478	0.0005	High	High	High
L2	2.82	4.18	5	409	0.0033	341	0.0040	High	Low	Low
H2	4.18	4.78	73	2012	0.0003	1206	0.0005	High	High	Moderate
H3	5.06	5.60	19	834	0.0006	1083	0.0005	Moderate	Moderate	High
L3	5.60	7.30	3	291	0.0058	425	0.0040	High	Low	Low
H4	7.30	7.60	41	804	0.0004	601	0.0005	Low	Moderate	High
L4	7.61	9.66	10	730	0.0028	515	0.0040	High	Moderate	Moderate

Notes: N = number of data points. Δt = sampling interval calculated by measurement intervals.

CHAPTER NOTE*

- N1. Kamikuri, S., Nishi, H., Motoyama, I., and Saito, S., submitted. Middle Miocene to Pleistocene radiolarian biostratigraphy in the Northwest Pacific, Ocean Drilling Program Leg 186, *Isl. Arc.*